Virtual outcrop-based analysis of channel and crevasse splay sandstone body architecture in the Middle Jurassic Ravenscar Group, Yorkshire, NE England

M. Mostafizur Rahman[1,2]*, John A. Howell[2] and David I. M. Macdonald[2]

[1] Department of Geology, University of Dhaka, Dhaka 1000, Bangladesh
[2] Department of Geology and Petroleum Geology, University of Aberdeen, AB24 3UE, UK
  MMR, 0000-0002-8867-571X
* Correspondence: mostafiz2021@du.ac.bd

Abstract: Well-exposed fluvio-deltaic deposits of the Middle Jurassic Ravenscar Group (Yorkshire coast) provide a direct analogue for North Sea reservoirs, but previous studies were restricted to a few accessible bays. This study used lidar and drone photogrammetry to create near-continuous virtual outcrops, 21 km long and 30–150 m thick, in an area which is largely inaccessible. Remote sensing data were supplemented by 45 outcrop logs and data from 27 pre-existing, behind-outcrop boreholes to improve understanding of the geometries, architectures and stacking patterns of 10 distinct sandbody types; the most important reservoir analogue units are channels and crevasse splay bodies. Channel bodies are 30–2038 m wide and 2–28 m thick with W/T ratio ranges of 5–105; the majority are multi-storey with an average thickness of 8 m and width of 182 m, while the single-storey channel bodies average 4 m thick and 50 m wide. Crevasse splays are 15–>1285 m wide and 0.3–6.5 m thick with W/T ratio ranges of 50–>541. There is a marked lateral and vertical change in channel body dimensions and facies proportion. The study suggests that the channel architecture and depositional nature of these successions are controlled by base-level fluctuation and floodplain topography.

Fluvio-deltaic sandstones act as significant petroleum reservoirs around the world (Tyler and Finley 1991; Keogh *et al.* 2007; Ford and Pyles 2014). Heterogeneity within these reservoirs exists at a variety of scales from the laminae to the basin fill although the main challenges typically exist at the architectural element scale (Keogh *et al.* 2007). The fluvial architecture describes the stacking of channel and overbank sandbodies and their geometry and interconnectedness (Allen 1978). Understanding and predicting fluvial architecture is key to understanding reservoir heterogeneity which has important economic implications as these deposits act as petroleum reservoirs, groundwater aquifers and potential sites for CO_2 sequestration (Campbell 1976; Miall 1988; Eschard *et al.* 1992*a*; Eaton 2006; Choi *et al.* 2007; Keogh *et al.* 2007, 2014; Ambrose *et al.* 2008; Nichols *et al.* 2011; Issautier *et al.* 2013; Owen *et al.* 2017). To date the majority of studies have focused on the stacking of channel sand bodies (e.g. Friend *et al.* 1979; Allen 1983; Blakey and Gubitosa 1984; Hirst 1991; Alexander 1992*a*; Alexander and Gawthorpe 1993; Bridge and Tye 2000; Gouw and Berendsen 2007; Jensen and Pedersen 2010; Sahoo *et al.* 2020), while overbank crevasse splay deposits have received less attention despite the fact that they can be both economically important and represent a key part of any holistic study of the fluvial system (Bown and Kraus 1987; Farrell 1987; Kraus 1987; Mjøs *et al.* 1993; Smith and Perez-Arlucea 1994; Willis and Behrensmeyer 1994; Miall 1996; Tooth 2005; Hajek and Edmonds 2014). The sedimentology of crevasse splay deposits has been studied both in modern fluvio-deltaic settings (Elliott 1974; O'Brien and Wells 1986; Farrell 1987; Bristow *et al.* 1999; Li *et al.* 2015) and ancient sedimentary rocks (Fielding 1984; Platt and Keller 1992; Jones and Hajek 2007;

Widera 2016; Burns *et al.* 2017). However, there are few quantitative and architectural studies of crevasse splays. Notable exceptions include studies by Smith (1993) and Gulliford *et al.* (2017) in the Lower Beaufort Group, Mjøs *et al.* (1993) in the Ravenscar Group, Jorgensen and Fielding (1996) in the Callide Coal Measures, van Toorenenburg *et al.* (2016) in the Huesca fluvial fan, and Burns *et al.* (2017) in the Castlegate Sandstone and Neslen Formation.

Overbank deposits record significant information on the environment and palaeoclimate at the time of deposition, especially as they typically contain a more complete stratigraphic record than the associated channel deposits (Bridge 1984; Fielding 1984; Kraus 1987; Demko *et al.* 2004; Lazar *et al.* 2015; van Toorenenburg *et al.* 2018). Overbank systems can also be relatively sand-rich when they are crevasse splay-prone and contribute to net reservoir/aquifer volumes and improve reservoir communication (Mjøs *et al.* 1993; Doyle and Sweet 1995; Anderson 2005; Pranter and Sommer 2011; van Toorenenburg *et al.* 2016, 2018). The character of overbank deposits, the presence and maturity of palaeosols and the vertical stacking of different facies (e.g. fining or coarsening upward) provide insight into the shifting position of the concurrent fluvial channel (Bown and Kraus 1987; Slingerland and Smith 2004; van Toorenenburg *et al.* 2016; Burns *et al.* 2019). The nature of overbank deposits is useful for predicting the style of channel avulsion, which has a strong influence on fluvial stratigraphy and the sandbody architecture (Jones and Hajek 2007; Hajek and Edmonds 2014). Detailed study of the channel bodies in conjunction with the associated overbank deposits provides a clear picture of the palaeodeposition systems, sandbody

distributions and their architectures (Fielding 1984; Bown and Kraus 1987; Kraus 1987). The present research focuses on a 40 km long, 30–150 m thick series of outcrops which expose the fluvio-deltaic deposits of the Middle Jurassic Ravenscar Group along the Yorkshire coast between Kettleness and Scarborough South Bay (Fig. 1). The three fluvial formations within the Ravenscar Group are each between 45–65 m thick and include channel sandstones, crevasse splays and floodplain mudstones which were deposited under a humid, subtropical climate in an alluvial to deltaic and paralic setting (Alexander 1992a; Morgans *et al.* 2017). These formations have been used as an analogue for hydrocarbon reservoirs, especially the similar aged Ness Formation which is part of the Brent Group in the North Sea (Hancock and Fisher 1981; Dreyer *et al.* 1990; Alexander 1992a and references therein; Butler *et al.* 2005).

Whilst these sections have been previously studied from a sedimentological (Hemingway and Knox 1973; Leeder and Nami 1979; Livera and Leeder 1981; Alexander 1992a; Ielpi and Ghinassi 2014) and reservoir analogue (Ravenne *et al.* 1987; Eschard *et al.* 1992a; Alexander and Gawthorpe 1993; Mjøs *et al.* 1993; Mjøs and Prestholm 1993) perspective, the previous work has focused on a limited number of accessible sections based on field observations and photomosaics taken from boats while the majority of the cliffs

have been inaccessible. Moreover, outcrops studied by two-dimensional photomosaics and/or scaled outcrop sketches, and the correlation between field logs, cannot account for the natural rugosity of exposures and introduces errors in the measurement of sizes and orientations of geobodies (Rittersbacher *et al.* 2014). In the current study these shortcomings have been addressed by using virtual outcrop data acquisition techniques as an addition to traditional field data collection (Buckley *et al.* 2010; Hodgetts 2013; Rittersbacher *et al.* 2014; Buckley *et al.* 2019).

The current study is designed to holistically address the fluvial/fluvio-deltaic system including both the channel and overbank deposits to provide a better understanding of the depositional history and controls on sandbody architecture and the associated heterogeneities The study used modern, virtual outcrop methods (Enge *et al.* 2007; Buckley *et al.* 2008) to provide additional insight into the geology of the entire depositional system by linking virtual outcrops with sedimentary logs from outcrops and behind outcrop boreholes. Specifically, the present research aims to improve understanding of the fluvio-deltaic sandbody architecture in these sections through (i) examining the fluvial facies in terms of their detailed sedimentology, stacking patterns and proportion; (ii) quantifying the channel and crevasse splay body dimensions; (iii) identifying vertical and lateral trends in sandbody dimensions to
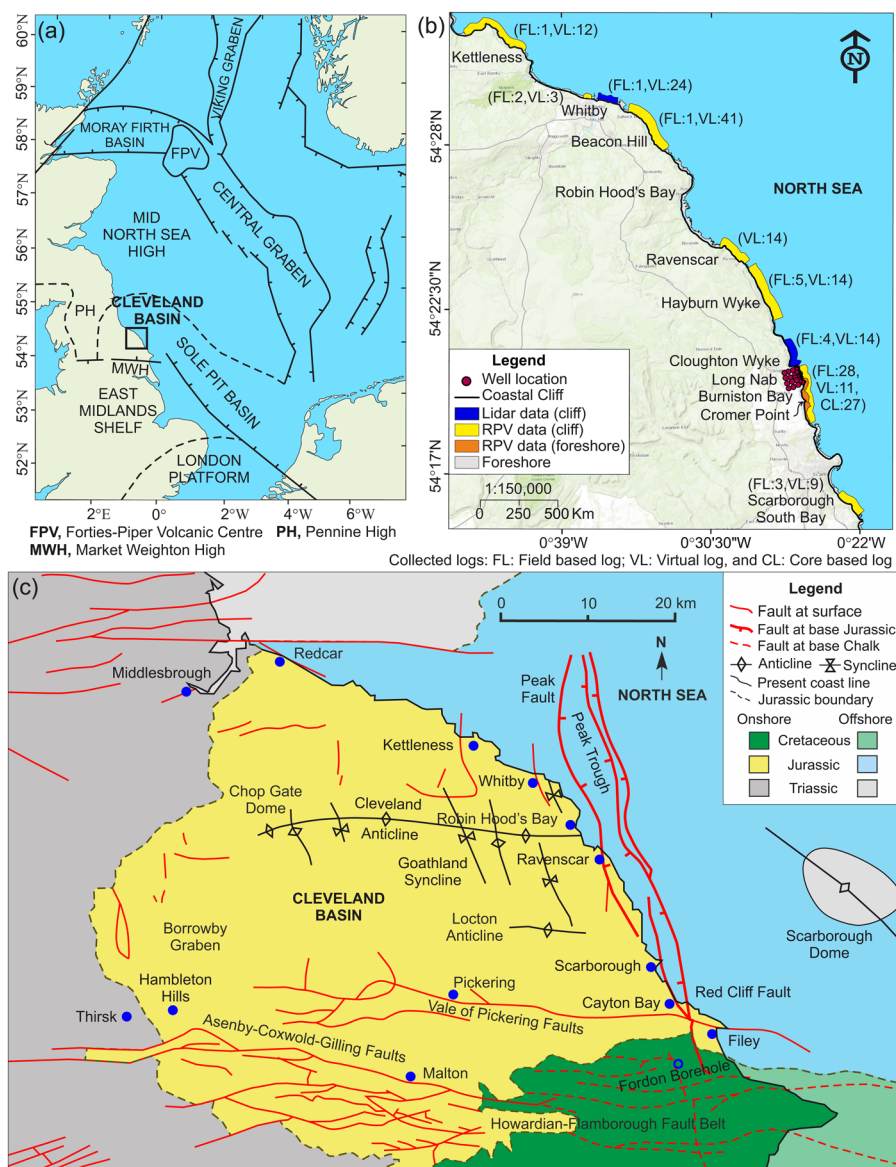

Fig. 1. (a) Generalized Jurassic palaeogeographic setting (after Powell 2010, p. 24, fig. 2). The black box represents the study area. (b) Location map showing the data collection sites between Kettleness and Scarborough South Bay along the Yorkshire Coastal Cliff Section. (c) Major structural setting of the Cleveland basin (modified after Kirby and Swallow 1987; Milsom and Rawson 1989; Kent 1980).

improve understanding on controlling factors; and (iv) analysing the architecture of overbank sandbodies and their role in paralic reservoir.

Geological setting and stratigraphy

The Ravenscar Group was deposited in the Cleveland Basin during the Middle Jurassic (Aalenian–Bathonian) (Hemingway and Knox 1973; Lott and Humphreys 1992; Cox and Sumbler 2002). The basin formed in the Jurassic as a part of a system of shallow epeiric seas and small extensional basins which linked to the North Sea Basin via the Sole Pit Trough (Fig. 1a). The Cleveland Basin was relatively small and was bounded to the NE by the Mid-North Sea High and the Pennine High to the west. The East Midland Shelf lay to the south of the basin, the northern part of which was comprised of the Market Weighton High (Kent 1955). The basin formation began in the Late Triassic as a result of differential subsidence and continued into the Cretaceous; by the Late Cretaceous active subsidence had halted and inversion began in the Early Neogene (Kent 1980; Kirby and Swallow 1987; Rawson and Wright 1992).

The Cleveland Basin lies to the south of the Mid-North Sea High and the major Early to Middle Jurassic thermal dome which uplifted the central North Sea (Sellwood and Hallam 1974; Ziegler 1982; Underhill and Partington 1993). Middle Jurassic sedimentation in the Cleveland Basin was characterized by progradation of fluvio-deltaic systems away from the thermal dome region toward the south and marine transgressions advanced in a north to northwesterly direction across the Market Weighton High (Hemingway 1974).

A number of regional-scale extensional and probable strike-slip fault complexes affected the Cleveland Basin (Hemingway 1974; Kirby and Swallow 1987; Fig. 1c). The east–west-trending Asenby–Coxwold–Gilling Graben, the Helmsley–Filey Fault Belt and the Howardian–Flamborough Fault Belt (defining the Vale of Pickering) were intermittently active to the south of the basin before the Market Weighton High formed during Mid- to Late Jurassic times (Kirby and Swallow 1987; Wright 2009). North–south-trending structures, such as the Peak Trough and Peak Fault (Milsom and Rawson 1989), the Cayton Bay Fault and the Whitby Fault cut the eastern margin of the basin. The Peak Trough contains thick Lower Jurassic rocks, suggesting that faults were at least active then (Hemingway 1974; Milsom and Rawson 1989). Late Toarcian regional uplift initiated by volcanic activity in the Central North Sea was associated with the development of the Mid-Cimmerian Unconformity which removed the upper part of the Lias Group across the basin (Black 1934; Hemingway 1974; Underhill and Partington 1993).

A number of the major bounding faults, especially the east–west-trending Coxwold–Gilling and Howardian–Flamborough fault belts, are known to have been active during the Cimmerian Orogeny which showed extension in the Oxfordian (Wright 2009) and renewed movements in post-Cretaceous times (Kirby and Swallow 1987; Starmer 1995). Petrographic and fission-track analysis suggest that prior to the inversion and north–south compression during the latest Cretaceous–Neogene, the Middle Jurassic sediments were buried to a depth of about 2–3 km (Hemingway and Riddler 1982; Green 1986; Bray et al. 1992). The inversion and north–south compression formed the complex east–west-trending Cleveland Anticline (Fig. 1c) and subsidiary folds including the Lockton Anticline, Goathland Syncline and Robin Hood's Bay Dome (Kent 1980).

The Ravenscar Group is comprised of marginal to non-marine clastics, thin coals and ironstones which are intercalated with relatively thin marine units of variable lithology. The maximum thickness is about 230 m in the Ravenscar to Scarborough section, thinning westward to 114 m in the Hambleton Hills and southwards to 57 m in the Fordon Borehole (Fig. 1c; Hemingway and Knox 1973; Powell 2010). The Ravenscar Group is composed of five formations: the Saltwick, Eller Beck, Cloughton, Scarborough and Scalby formations. The Saltwick, most of Cloughton, and Scalby formations are generally considered to be delta plain deposits (Hancock and Fisher 1981; Livera and Leeder 1981; Alexander 1992a). The delta plain deposits are separated by three distinct transgressive marine units: the Eller Beck Formation, the Lebberston Member of the Cloughton Formation, and the Scarborough Formation (Hemingway and Knox 1973; Livera and Leeder 1981; Fig. 2).

The lowermost part of the Ravenscar Group, the Aalenian Saltwick Formation, unconformably overlies the marine Dogger Formation. In places, where the Dogger Formation is absent, it rests unconformably on the Alum Shale of the Lias Group. The Saltwick Formation is comprised of channel sandstones, crevasse splays and floodplain mudstones (Alexander 1992a). The Saltwick Formation is overlain by shallow marine deposits of the Eller Beck Formation (Knox 1973). This unit has a conformable base and coarsens upward. It comprises thin beds of ironstone near the base to mudstone and finally fine- to medium-grained planar to low-angle cross-stratified, and wave-rippled sandstone (Knox 1973; Hemingway 1974; Livera and Leeder 1981). The presence of rootlets at the uppermost part of the sandstone suggests emergence and the unit passes gradationally into the overlying fluvio-deltaic deposits of the Cloughton Formation (Livera and Leeder 1981). The Cloughton Formation is lithologically similar to the Saltwick Formation except for the presence of the marine limestone/sandstone unit of the Lebberston Member in the south of the basin, which divides the formation into the lower Sycarham Member and upper Gristhorpe Member (Powell 2010). The Scarborough Formation conformably overlies the Cloughton Formation and comprises a wide range of deposits including sandstones, mudstones, argillaceous limestone and different types of mixed siliciclastic/carbonate sediments (Hemingway and Knox 1973; Cope et al. 1980; Gowland and Riding 1991).

Overlying the Scarborough Formation is a succession of channel sandstones, crevasse splay sandstones and floodplain mudstones of the Scalby Formation which demonstrate the return of fluvio-deltaic and paralic depositional settings (Leeder and Nami 1979). The lowermost c. 9 m of the formation consists of fine- to medium-grained, locally pebbly, cross-bedded channel sandstones termed the Moor Grit Member, which rests unconformably on the Scarborough Formation (Nami 1976; Nami and Leeder 1978; Leeder and Nami 1979; Ielpi and Ghinassi 2014). The Moor Grit is overlain by the exhumed meander belt deposits, and delta plain channel and overbank deposits of the Long Nab Member (Nami 1976; Alexander 1992b; Ielpi and Ghinassi 2014).

Data and methods

Data were collected by traditional field observations, terrestrial lidar scanning, and RPV (remotely piloted vehicle, drone) photogrammetry (Howell et al. 2021) from a 40 km section of the coast. Sections are between 30 and 150 m thick. The sections are subdivided into nine outcrops (Fig. 1b), which are separated by areas of no-exposure, or in the case of Robin Hood's Bay, by an anticline which brings older Dogger Formation deposits to the surface. A total of 45 sedimentary logs were measured at accessible outcrop localities (at least one log per outcrop except Ravenscar; Appendix A) to calibrate the virtual outcrops and to document the lithological variation, sedimentary structures, ichnofacies and palaeocurrent. Detailed sandbody architectures were sketched on photo-panels in the field and then on virtual outcrops in the lab using the LIME software (Buckley et al. 2019). In addition, more than 800 m of core from 27 boreholes were also logged in the National Geosciences Data Centre and the British Geological
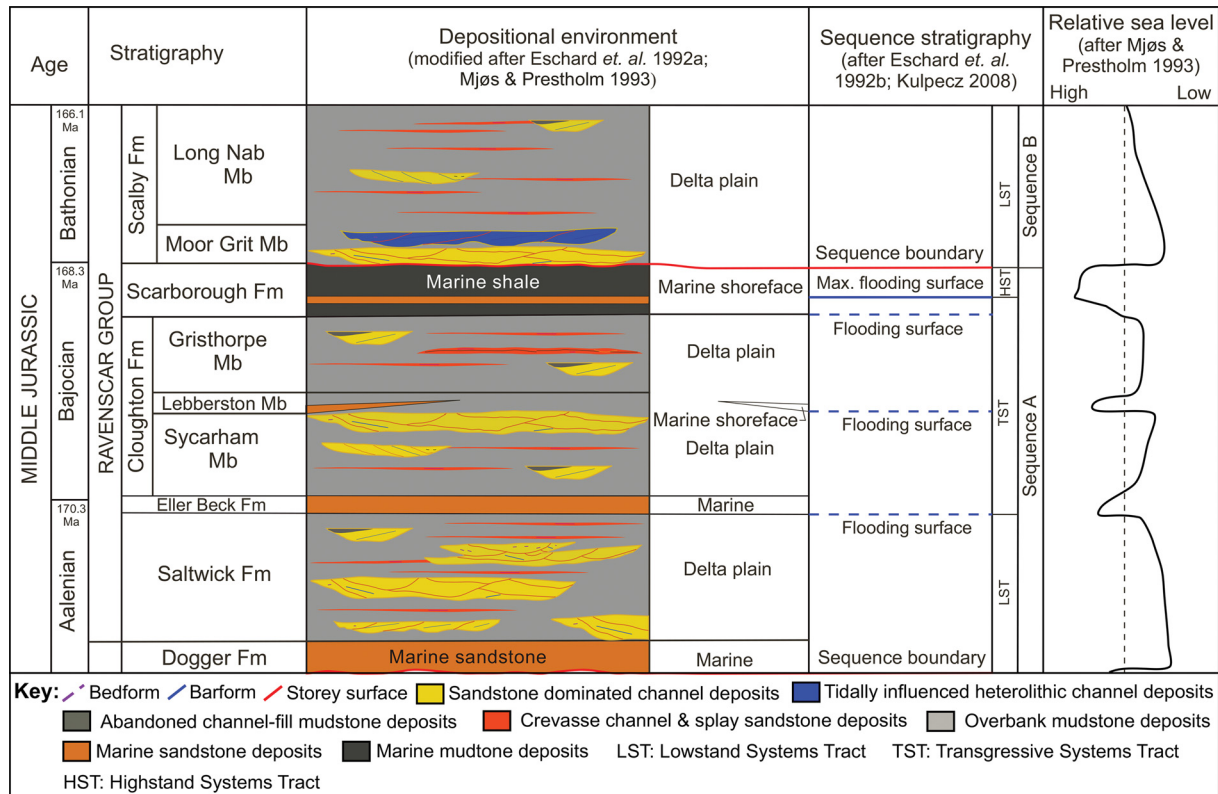
Fig. 2. Generalized stratigraphic table of the Ravenscar Group with the depositional environment and sequence stratigraphic units (modified after Eschard *et al.* 1992*a*, *b*; Mjøs and Prestholm 1993; Kulpecz 2008).

Survey, UK. These behind-outcrop boreholes are clustered near the Long Nab outcrop at Cloughton Bay and were drilled by Institut Francais du Petrole in the late 1980s. The boreholes are 30–50 m deep and sampled the Scalby Formation and uppermost part of the Scarborough Formation (Eschard *et al.* 1992*a*). Sedimentary logs from the borehole cores were prepared at the scale of 1:50 with detailed descriptions of grain size (Wentworth Scale), texture, colour, compaction, grain sorting, bed thickness, sedimentary structures and bioturbation index with characteristic trace fossils (Appendix B).

Ground-based lidar scanning was performed at the Whitby East and Cloughton Wyke sections following the methodologies outlined in Buckley *et al.* (2008) and Enge *et al.* (2010). RPV (drone) photogrammetry was used at Kettleness, Whitby West, Beacon Hill, Ravenscar, Long Nab and Scarborough South Bay cliff sections using the methodology outlined in Howell *et al.* (2021). Lidar and RPV data were used to build scaled photorealistic models (virtual outcrops; Appendix C) from which sandstone body geometry (e.g. width, thickness), stacking pattern, distribution and average lithofacies were studied. The virtual outcrops (VOs) provide a spatially accurate three-dimensional representation of the outcrop (Fig. 3).

The VOs were imported into LIME, a software for VO interpretation (Buckley *et al.* 2019) to visualize and interpret the sections. Sandbodies were each mapped with polylines and given a unique name. Their width and thickness were measured, as well as the outcrop orientation, a qualifier for their completeness (complete when the full sandbody is exposed, and incomplete when the sandbody is partially exposed, i.e. the sandbody dimension is greater than the outcrop extent) and a description of the lithology and architectural elements present. The measured width refers to a minimum observed value and includes jump correlation across small (<50 m) gaps in the exposures (Rittersbacher *et al.* 2014). The length of the direct line between the two outermost points of the sandbody is considered as its apparent width (Gouw and Autin

2008) which is then corrected for obliquity following the approach of Fabuel-Perez *et al.* (2009). In this method, the angle of the exposed sandbody was combined with the palaeoflow direction to calculate the true width of the sandbody (Appendix C). Due to the inaccessibility of most of the cliff sections, regional palaeoflow directions for each formation, collected from sedimentary structures in the field and published studies, were used rather than measurements from individual sandbodies. The mean palaeocurrent direction of the Saltwick channel bodies is towards 182° (n = 56) and the Scalby channel bodies towards 170° (n = 57). No palaeocurrent data were measured for the Cloughton Formation and the average palaeocurrent data of this formation was adopted from Livera (1981) as towards 194°. The thicknesses of the sandbodies and the formations were measured vertically keeping the VO horizontal to overcome the measurement error due to slight tectonic dip of the sections. Several measurements were taken at an equal distance for each sandbody to record their maximum and average thicknesses.

The dimensions of crevasse splay deposits were also measured from VOs and where possible in the field. An associated study of modern systems (Rahman 2019, ch. 2) suggests most of the splays are generated at around 90° to the channel flow direction. Therefore, regional palaeocurrents were also used to correct apparent widths measured from the outcrops (Appendix C). Thickness data for the splays were based upon a minimum of 10 equidistant measurements along the splay and maximum, mean and minimum thicknesses were recorded. For both channel and splay deposits, the height of the top of the unit above the base of the respective formation was also recorded as a stratigraphic datum in a similar manner to the method used by Rittersbacher *et al.* (2014).

Pseudo-logs also known as virtual logs were generated from the VOs to study the lateral facies variation away from the outcrop measured sections. A total of 142 pseudo-logs were generated with a typical spacing of 200 m. These included 96 from the Saltwick
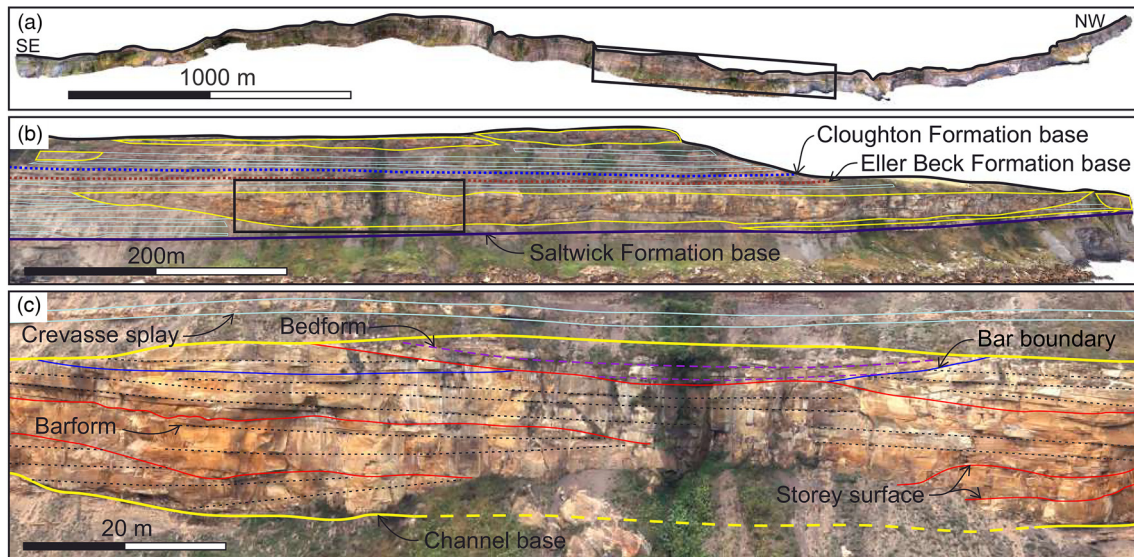
Fig. 3. Example of a typical virtual outcrop (VO) used in this study. (**a**) VO of Beacon Hill Cliff section (see Fig. 1 for location). (**b**) Detail of part of (**a**) (see black box) depicting the fluvial architecture and formation boundaries. The yellow-bordered features are channel body and the light grey features are crevasse splay bodies. (**c**) Further detail (see box in (**b**)) showing the bedform and bar form scale interpretation. Red lines represent the storey surfaces, blue lines the bar boundaries; black dotted lines within bars are the lateral accretion surfaces, and broken pink lines are bedding surfaces.

Formation, 26 from Cloughton Formation and 20 from the Scalby Formation (Fig. 4). The thicknesses of different sandbodies and separating mudstones were recorded so that the sand/mud (equivalent to the net/gross ratio) ratio could be quantified.

Facies analysis

Facies characteristics of the fluvial successions were studied from sedimentary logs (Fig. 5) collected from the outcrop and borehole sections. A total of 24 lithofacies were identified in the fluvio-deltaic successions of the Ravenscar Group, which are summarized in Table 1 and Figure 6. The lithofacies were grouped into seven facies associations which were further grouped into those that form within the channels and those that form in the overbank environment (Table 2 and Figs 7 and 8). The associations are described below.

Channel deposits

Large-scale erosive-based bodies are generally comprised of coarse sediments deposited within the channels. Channel deposits
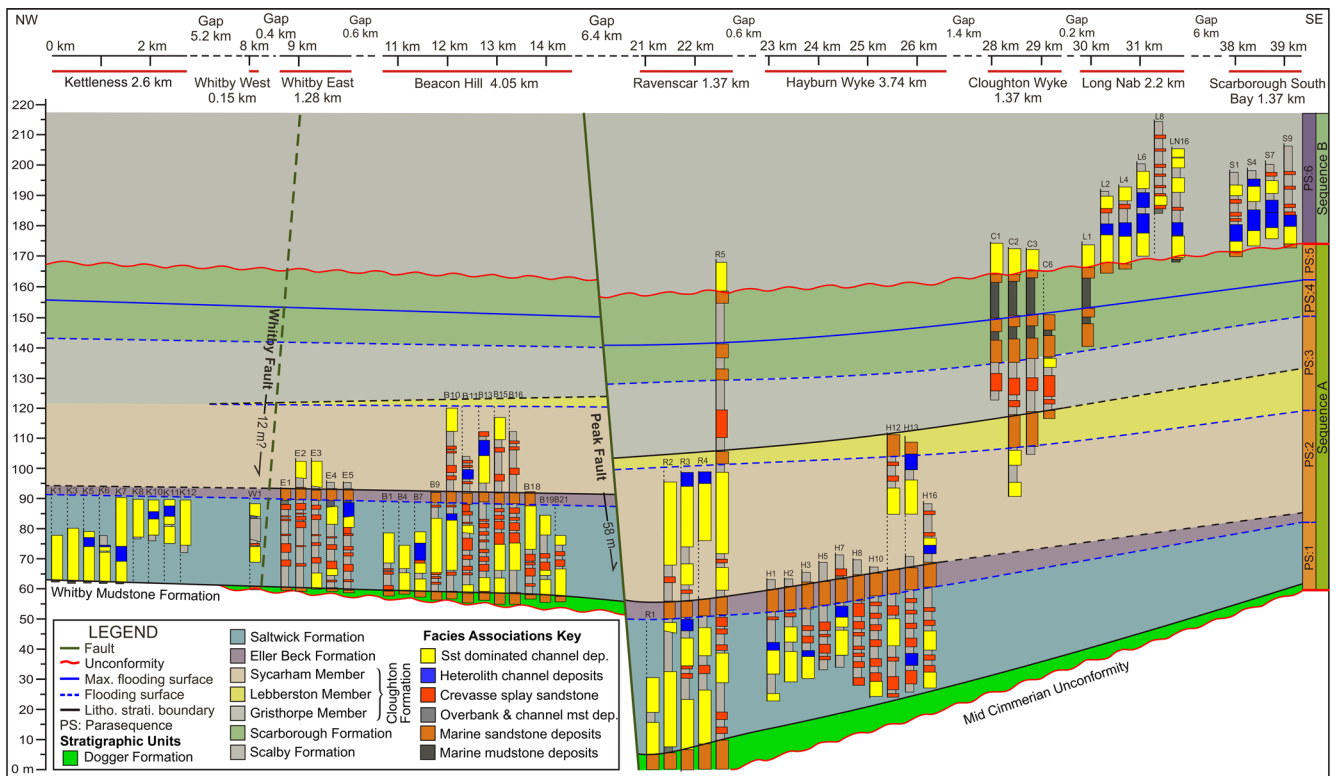

Fig. 4. Schematic representation of the distribution of lithofacies based on virtual logs between Kettleness and Scarborough South Bay, a 40 km long section. The outcrop and core-based sedimentary logs were also considered in preparing the panel. Formation thickness adopted from Hemingway (1974) where formation top/base is not exposed and in the case of a data gap.
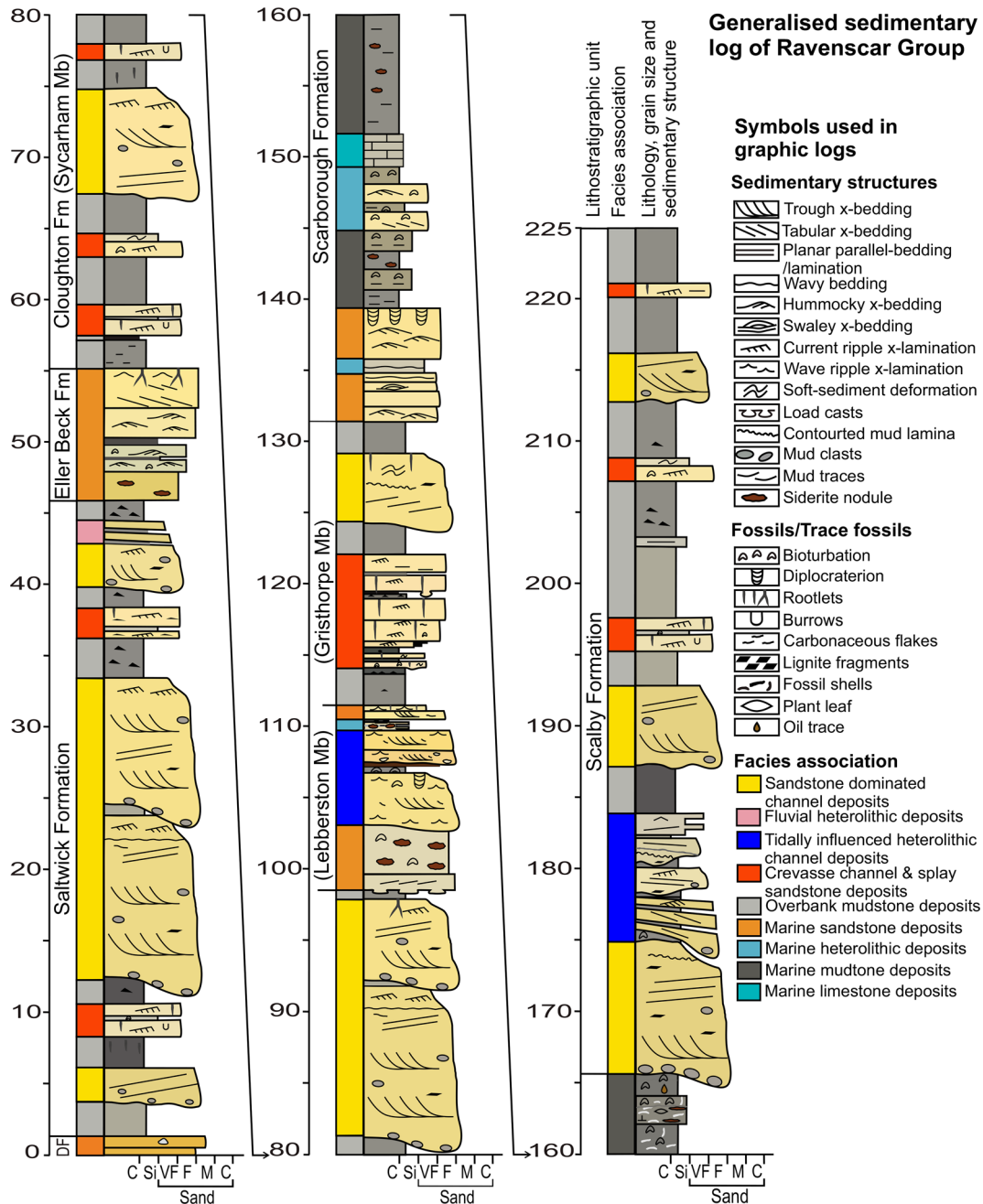
Fig. 5. Generalized sedimentary log of the Ravenscar Group. Fluvial successions are based on measurement of accessible outcrops along the coastal cliff, behind outcrop borehole core and VOs. The marine successions are based on VOs and after Hesselbo *et al.* (2003).

are categorized into three facies associations based on their lithological characteristic. The channel–storey and stacking patterns are described in the subsequent sandbody architecture section.

Facies association 1 (FA1): sandstone-dominated channel deposits

Facies association 1 (FA1) is mostly comprised of the accretionary bar, and aggradational channel sandstone. The deposits occur in accretionary barforms that are up to 8 m thick and 120 m long. Stratal dips within the bar forms are between 7–25° (Fig. 7a, b). Strata with the accretionary sets typically have a uniform dip and are separated from similar bar forms within the same sandbody by minor erosion surfaces and a change in dip direction and angle. Palaeocurrents within the bar forms are oblique (>60° angle) to

perpendicular to the dip of the strata. Aggradational channel deposits are generally 1.5–3 m thick. In multi-storey sandbodies, they are generally observed at the basal part and are eroded by the accretionary bars; however, they are also observed besides the accretionary bars (Fig. 7b). This facies association consists of grey to yellowish grey, fine- to medium-grained sandstone with rare locally persistent intraformational conglomerate observed at the base of the sandbodies. Sandstones display tabular, trough, low-angle cross-stratification and ripple cross-stratification with some massive and rarely sigmoidal cross-stratification. The cross-beds contain mud pebbles, carbonaceous and mudstone drapes, and wood fragments converted to coal (up to 30% in a few places). Cross-bed set thickness decreases upward from more than 1 to 0.1 m. Locally 10 cm to meter-scale syn-depositional minor faults were observed in both the core and outcrop sections. Slumped and water-escaped structures were also occasionally present.

Table 1. *Lithofacies scheme of studied fluvio-deltaic successions in the Middle Jurassic Ravenscar Group*

| Code	Facies	Lithology	Biogenic content	Basal contact	Process of deposition
C_{IF}	Intraformational conglomerate	Pebble to granule-sized mud clasts and medium-grained sandstone, flooring erosional surface	Not observed	Erosional	Reworking of lag deposits after erosion
S_M	Massive sandstone	Yellowish grey sandstone with lignite fragments and mud pebbles	Occasionally contain lignite fragments	Erosional/flat sharp	Rapid deposition from suspension during floods
S_{LXS}	Low angle cross-stratified sandstone	Yellowish grey sandstone with lignite fragments and mud pebbles	Occasionally contain lignite fragments	Erosional/flat sharp	Migration of sand sheet or 2D dunes
S_{RXS}	Current ripple cross-stratified sandstone	Light grey to yellowish grey sandstone frequently with lignite fragments	Occasionally contain lignite fragments	Flat deposition surface	Migration of current ripples
S_{WRXS}	Wave ripple cross-stratified sandstone	Light grey to yellowish grey sandstone with carbonaceous drapes and lignite fragments	Occasionally contain very thin carbonaceous/mud drapes	Wavy based	Migration of wave ripples
S_{TbXS}	Tabular cross-stratified sandstone	Yellowish grey to dusky yellow sandstone frequently with mud pebbles and lignite fragments; occasionally with carbonaceous/mud drapes	Occasionally contain lignite fragments	Erosional with scour marks or flat sharp	Straight/long crested dune migration
S_{TXS}	Trough cross-stratified sandstone	Yellowish grey sandstone frequently with lignite fragments and mud pebbles; occasionally with carbonaceous/mud drapes	Occasionally contain lignite fragments	Erosional with scour marks or flat sharp	Curve crested dune migration
S_S	Slumped sandstone	Yellowish grey fine-grained sandstone with lignite fragments	Occasionally contain lignite fragments	Erosional/flat sharp	Slumping
S_{PPS}	Planar parallel stratified sandstone	Yellowish grey sandstone with carbonaceous drapes or mud drapes	Occasionally contain lignite fragments	Erosional or flat sharp	Upper stage plane bed transport
S_{SXS}	Sigmoidal cross-stratified sandstone	Grey sandstone with lignite fragments	Occasionally contain lignite fragments	Flat sharp based	Washed out dune
S_{WF}	Sandstone with abandoned wood fragments	Grey to yellowish grey structureless sandstone with abundant wood fragments of various sizes. The wood fragments are converted into coal.	Contains abundant wood fragments	Sharp	Both accretion and channel fill
HS_B	Bioturbated sand-dominated heterolithic	Grey to yellowish grey fine-grained sandstone and alternated mudstone	Bioturbation including burrowing traces	Flat surface	Suspended settling with weak current
HS_S	Deformed sand-dominated heterolithic	Grey to yellowish grey fine-grained sandstone and alternated mudstone deformed by water escaping or slumping	Occasionally contain lignite fragments	Flat surface	Suspended settling with weak current and modified by slumping/water escaping
HM_B	Bioturbated mud-dominated heterolithic	Grey to yellowish grey mudstone and silty sandstone	Bioturbation and burrowing traces	Flat surface	Suspended settling with weak current
HM_S	Deformed mud-dominated heterolithic	Medium grey to yellowish grey mudstone and silty sandstone	Occasionally contain bioturbation	Flat surface	Suspended settling with weak current modified by slumping/water escaping
H_{FS}	Flaser stratified	Yellowish grey sandstone with dark grey to black organic-rich mudstone in the ripple trough	Root traces and occasional bioturbation	Irregular surface	Deposited by current flow and from suspension
H_{WS}	Wavy stratified	Yellowish grey rippled sandstone with dark grey mudstone drapes	Bioturbation	Irregular surface	Deposited by alternating current flow and suspension
H_{LS}	Lenticular stratified	Yellowish grey isolated rippled sandstone in dark grey mudstone	Bioturbation	Irregular surface	Deposited by decaying current flow and suspension
M_M	Massive mudstone	Light grey to dark grey mudstone	Occasionally contain carbonaceous fossil plant fragments, plant roots, leaf etc.	Flat surface	Suspension
M_L	Interlaminated mudstone	Light grey to dark grey mudstone	Occasionally contain carbonaceous fossil plant fragments, plant roots, leaf etc.	Flat surface	Deposition from suspension or very low energy underflows
M_B	Bioturbated mudstone	Light grey to dark grey mudstone	Bioturbation and burrowing traces	Flat surface	Suspension
M_S	Slumped or deformed mudstone	Light grey to medium grey mudstone	Occasionally with carbonaceous matters	Flat surface	Deposition from suspension and modified by slumping/water escaping
S_{PSol}	Palaeosol	Greyish brown to blackish red soil	Often with carbonaceous matters and rootlets	Flat surface	Suspension followed by pedogenesis
C	Coal	Very thin locally extended black coal within channel fills or overbank pond fills	Plant woods	Very thin concave up	Allochthonous coal or highly carbonaceous mud deposited from suspension in abandoned channel/overbank ponds
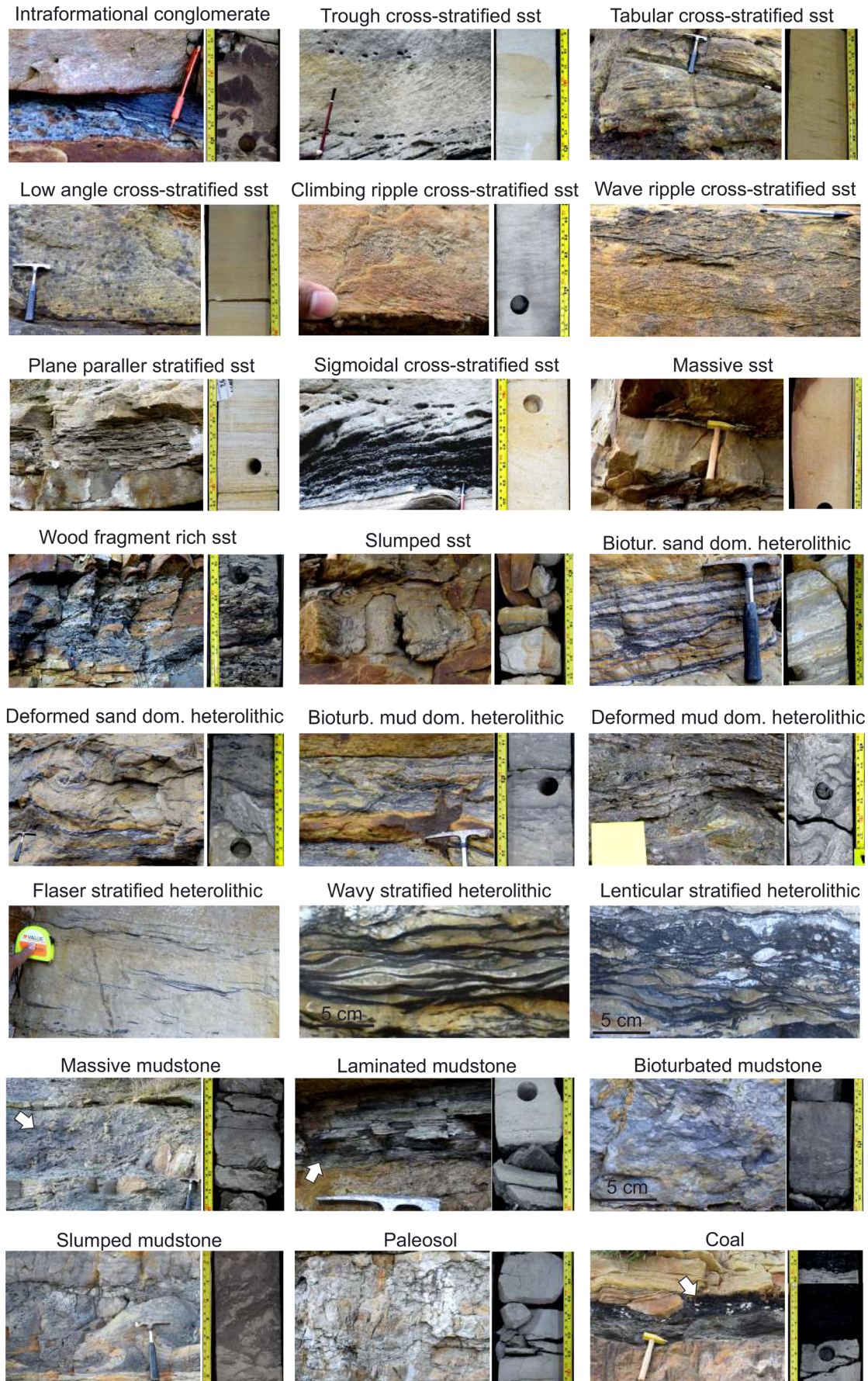
Fig. 6. Photographic examples of lithofacies in fluvio-deltaic successions of the Middle Jurassic Ravenscar Group. The same facies scheme has been used to both in the outcrop and subsurface core interpretation. Lithofacies descriptions and interpretation are in Table 1.

| Lithofacies association	Facies	Description	Ichnofossils and biogenic structures	Geometry	Environmental interpretation
Channel deposits	FA1: Sandstone-dominated channel deposits	S_M; S_{TXS}; S_{TbXS}; S_{LXS}; S_{PPS}; S_{RXS}; S_{SXS}; S_{WF}; M_S; M_B; M_L	Clean fine- to medium-grained basal erosive surfaced massive, trough, tabular, low angle, sigmoidal, current ripple cross-stratified and plane-parallel-stratified fluvial channel sandstone with abundant rip-up clasts and lignite fragments. Occasionally there are wavy carbonaceous and mud drapes, thin laterally discontinuous mud layers and soft sediment deformations	Not observed	Multi-storey sheet and single storey ribbon	Clean fine- to medium-grained sandstone with cross-stratified nature indicates fluvial channel deposits. The multi-storey channel fill units demonstrate the channels eroded each other. The small ribbon channel bodies are the lower delta plain distributary channel
	FA2: Heterolithic channel deposits Sub-associations: FA2A: Fluvial heterolithic deposits FA2B: Tidally influenced heterolithic channel deposits	S_{TXS}; S_{TbXS}; S_{RXL}; S_S; M_S(CC); M_M(LF) FA2A: S_{TXS}; S_{TbXS}; S_{RXL}; S_S; S_B; H_{SW}; H_B; H_{FS}; M_S; M_B(CC); M_M(LF)	Composed of inclined heterolithic statifications (IHS). Two sub-associations are: FA2A and FA2B. FA2A: Fine-grained trough, tabular, and ripple cross-stratified sandstone and thin mudstone layers with occational soft sediment deformation stuctures. Rip-up-clasts and lignite fragments are also common FA2B: Fine-grained, trough, tabular and ripple cross-stratified; bioturbated, slumped sandstone; and flaser, wavy stratified bioturbated sand dominated heterolithics alternated by intensely bioturbated mudstone layers with carbonaceous and mud drapes, and *Acanthomorph Acritarchs* microfossils	Rare bioturbation Moderate–high bioturbation	Tabulat single sheet Single/multi-storey sheet	Alternating fine sandstone and mudstone layers, absence of abundant bioturbation and bidirectional sedimentary structures indicate fluvial heterolithic point bar deposits Interbedded sandstone and mudstone composition, abundant carbonaceous and mud drapes, bioturbation, and presence of saline water palynofacies indicate tidally influenced meandering channel deposits
	FA3: Mudstone dominated channel deposits	M_L	Plane-parallel-laminated mudstone with abundant millimetre-scale lignite fragments	Not observed	Single-storey ribbon	2 to 4 m thick parallel-laminated fining upward mudstone deposits with channel-shaped geometry suggests the abandoned channel fill deposit
Overbank deposits	FA4: Splay sheet and crevasse channel sandstone deposits Sub-associations: FA4A: Splay sheet deposits FA4B: Crevasse channel deposits	S_{RXS}; S_{PPS}; M_L; M_B; S_{TXS}; S_{TbXS};	Two sub-associations are: FA4A and FA4B. FA4A: Fine-grained current ripple cross- and planar-parallel-stratified sharp erosive based, rooted, 50–80 cm thick sheet sandstone alternated with planar-parallel-stratified 5–12 cm thick silty, bioturbated mudstone; rootlets and plant leaves are also common. FA4B: Fine to medium grained, tabular, and ripple cross-stratified, erosive based, ribbon sandstones	Moderate bioturbation in mudstone	Thin sheet and tiny ribbon	Fine-grained planar to ripple cross-laminated sandstone with sharp basal contact (fourth order?) over mudstone, plant roots and bioturbations indicate the crevasse splay deposits. Small ribbon shaped fine- to medium-grained tabular and ripple cross-stratified sandstone flanked with splay sheets indicate crevasse channel deposits
	FA5: Mudstone dominated heterolithic levee deposits	M_L; M_s; S_{RXS}; S_{WRXS}; S_{PPS}	Yellowish grey ripple cross (both current and wave) and plane parallel stratified silty fine-grained sandstone alternated with grey parallel-laminated and occasionally deformed mudstone	Not observed	Wedge-shape	Mudstone-dominated heterolithic composition, wedge-shaped geometry, unidirectional small-scale sedimentary structure and occurrence adjacent to the channel deposits suggest these are levee deposits
	FA6: Overbank mudstone deposits	M_L (CM); M_M; $M_{S,B}$	Grey and dark grey to black parallel-laminated, massive and bioturbated mudstone, occasionally with abundant organic matter	Moderate bioturbation, carbonaceous matters, and rootlets	Sheet	Laterally persistent, massive to parallel-laminated mudstone suggests overbank origin. Plane-parallel lamination, abundant organic matters and sporadic very fine sand laminal composition along with bioturbation indicate deposition in the subaqueous shallow water lakes or floodplain ponds. The grey massive to poorly laminated mudstone with rootlets at the bed top indicated subaerial floodplain deposits.
	FA7: Palaeosol	S_{Psol}	Greyish brown, mottled to blackish red colour and blocky texture	Extensive rootlets	Sheet	Presence of abundant roots, colour mottling, blocky texture etc. suggest subaerial exposure and pedogenesis
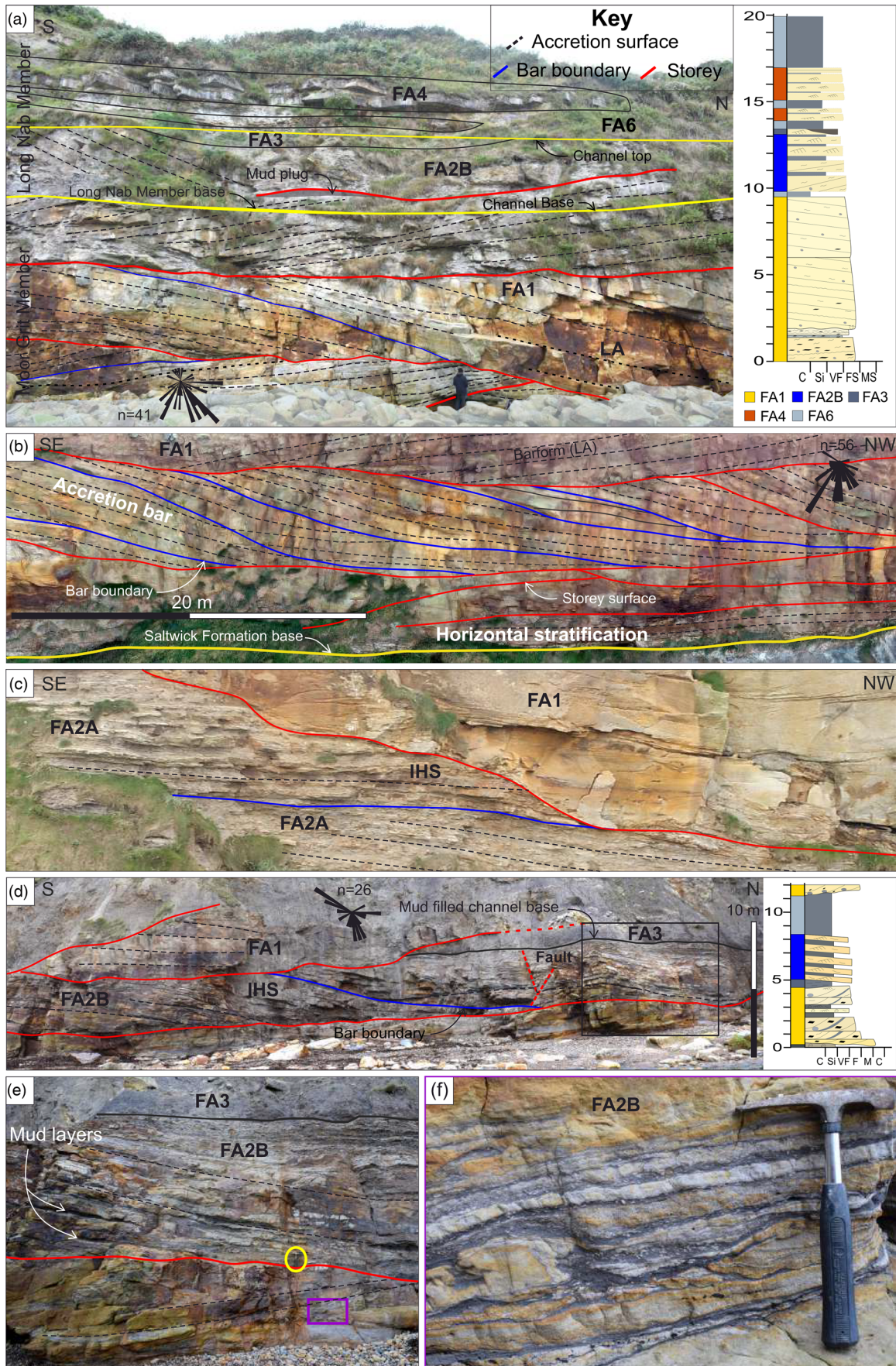
Fig. 7. Examples of facies associations. (**a**) The major facies associations in the Scalby Formation exposed *c.* 300 m south of Hundale Point; thick (*c.* 6 m), tabular cross-stratified, fine- to medium-grained sandstone in multi-storey channel deposits. (**b**) Detailed interpretation of FA1 in the Saltwick Formation exposed at the Kettleness section. (**c**) Fluvial inclined heterolithic stratification (inclined heterolithic stratification (IHS); FA2A) along with FA1 in the Saltwick Formation exposed at the Kettleness section. (**d**) Tidally influenced IHS (FA2B) in the Scalby Formation exposed at Scarborough South Bay. (**e**) Detail of the black box in (**d**) showing the repeated sandstone and mudstone layers alteration in IHS. (**f**) Detail of the purple box in (**e**) indicateing the bioturbation in mudstone layers.
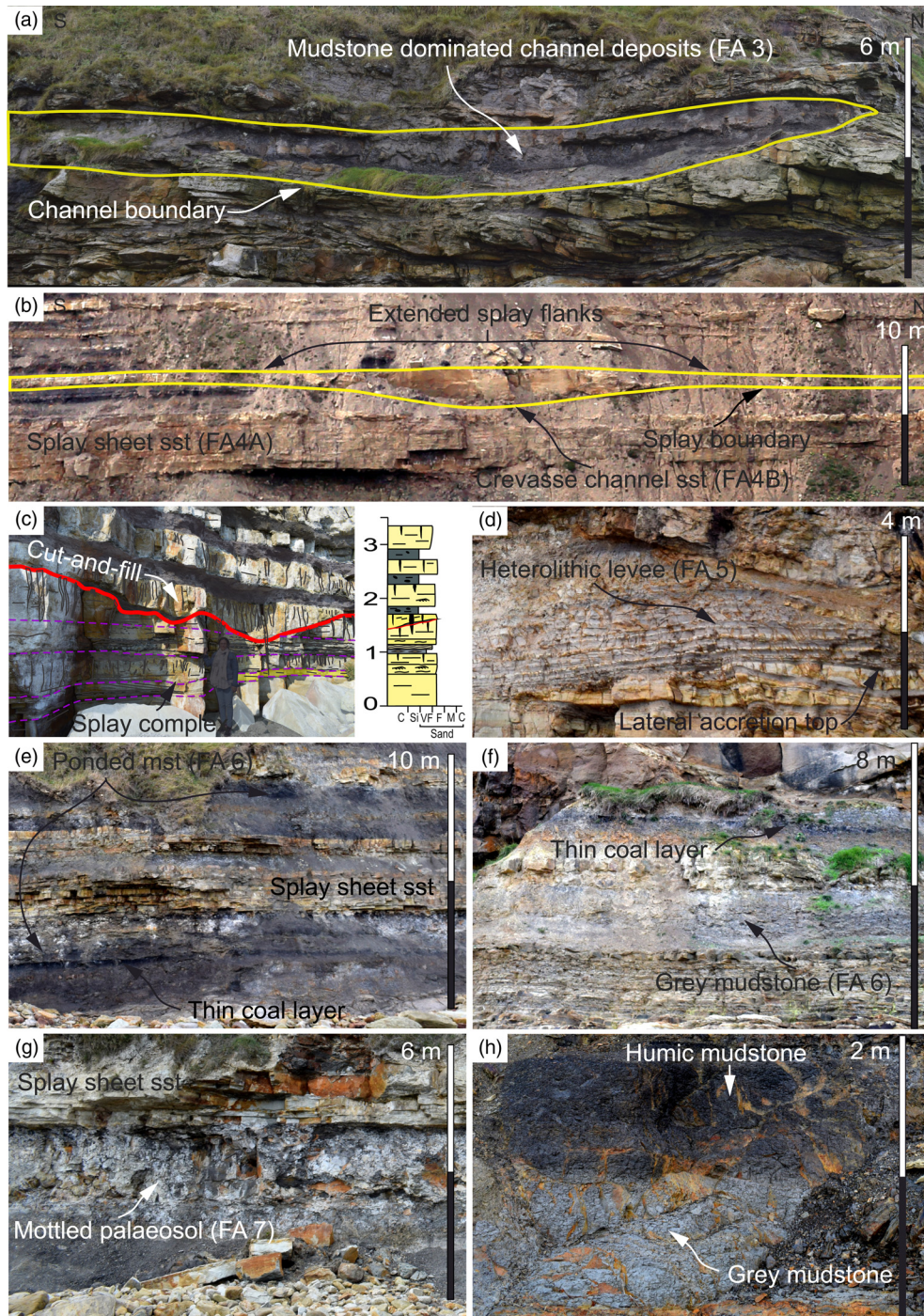
Fig. 8. Examples of the fine-grained channel, and overbank Facies Associations. (**a**) Mudstone-dominated channel deposits (FA3) associated with FA2 exposed north of Long Nab in the Scalby Formation. The main channel fill deposit is mudstone with an occasional thin lenticular fine-grained sandstone layer. (**b**) Small ribbon-shaped crevasse channel with extended splay sheet sandstone from the Saltwick Formation exposed at High Whitby. (**c**) Coarsening-upward splay complex deposits at Cloughton Wyke in the Gristhorpe Member and detailed sedimentology of interdistributary bay-fill splay complex with tidal sedimentary structures, cut and fill nature and traces of rooting. (**d**) Fining-upward heterolithic levee deposits on the top of the older channel bar deposits at Whitby West Cliff in the Saltwick Formation. (**e**) Shallow lake or ponded floodplain mudstone deposits at the South of Long Nab in the Long Nab Member. (**f**) Grey massive floodplain mudstone deposits at Whitby West Cliff in the Saltwick Formation. (**g**) Mottled palaeosol at Burniston Bay in the Long Nab Member. (**h**) Partial soil development in the coastal swamp deposits exposed at North of Hayburn Wyke in the lower part of the Saltwick Formation.

Bioturbation was not observed in the studied section except for the presence of rootlets in the channel top.

These bodies are interpreted as the deposits of large, dominantly meandering, fluvial channels. The horizontally stratified deposits, which make up a minor proportion of the succession, were deposited by the aggradation process in the base of vertically aggrading channels, while the bulk of the sedimentation took place within accretionary bars. The oblique (>60° angle) to perpendicular relationship between the accretion direction and the bedform palaeocurrent direction along with the lithofacies assemblage of the accretionary bars deposits indicate that these are lateral-accretion units deposited in the point bars (Miall 1996). Conglomerates at the base of channels represent bypass lags deposited during the cut of the channel while thick, intra-channel mud-clast conglomerates are the result of intraformational erosion and bank collapse.

Facies association 2 (FA2): heterolithic channel deposits

Facies association 2 (FA2) is composed of heterolithic lateral accretion elements, equivalent to inclined heterolithic stratification (IHS) of Thomas *et al.* (1987) and epsilon cross-stratification units of Allen (1963) and aggradational heterolithic fills (Fig. 7). Two types of heterolithic deposits are observed: fluvial heterolithic deposits (facies association 2A) and tidally influenced heterolithic channel deposits (facies association 2B).

Facies association 2A (FA2A): fluvial heterolithic deposits

Facies association 2A (FA2A) is composed of fine- to medium-grained trough, tabular and ripple cross-stratified sandstone, alternating with thin mudstone layers (Fig. 7c). Bioturbation was rarely observed in the studied sections. Soft sediment deformation consisting of slump structures, convolute lamination and water-escaped features was observed locally. Abundant rip-up clasts and lignite/coal fragments were also present. A lateral fining trend both toward and away from the depositing palaeochannel was present in several sections, interpreted as point bars.

The IHS successions are sharp or erosive-based, tabular shaped bodies which are 2–3.5 m thick and up to 120 m wide. The cross-strata are centimetre- to decimetre-scale thick and show a low dip, in the range 4–15°. The IHS sequences were generally observed at the top of FA1 and associated with FA3 and FA6. They were studied in the Saltwick Formation, exposed at the Kettleness, Whitby East and Beacon Hill sections.

IHS are typically deposited in point bars of sinuous meandering streams (Thomas *et al.* 1987). The alternation of mudstone and sandstone and the hierarchical arrangement reflect a superimposition of several distinct types of depositional events. The absence of abundant bioturbation and bidirectional sedimentary structures and the association with proximal delta plain deposits indicate no marine (tidal) influence. The observed characteristics suggest that the alternating sand and mud layers were deposited as a result of fluctuating discharge at the late stage of sinuous palaeochannels (McGowen and Garner 1970; Thomas *et al.* 1987).

Facies association 2B (FA2B): tidally influenced heterolithic channel deposits

Facies association 2B (FA2B) is also composed of alternating sandstone and mudstone layers with additional tidal imprints. The grain size ranges from fine- to medium-grained sandstone with abundant mud drapes and alternating bioturbated mudstone layers (Fig. 7d–f). FA2B exhibits a high bioturbation index (Taylor and Goldring 1993), up to BI 4 in mud layers and typically low in cross-stratified sandstones (BI 1). Inertinite-dominated palynofacies and rare *Acanthomorph Acritarchs* microfossils are reported by Fisher and Hancock (1985) in an exhumed meander belt of the Scalby Formation. Abundant rip-up clasts and lignite/coal fragments are also present.

Sandstone layers are trough, tabular and ripple cross-stratified; alternating mudstone layers are thinly laminated and bioturbated (Fig. 7e). Cross-strata dip from 9 to 25° and strike at 200–286°. Measured paleocurrent ranges from 008 to 354° (average 170°). Soft sediment deformation structures are also observed in both sandstone and mudstone strata. The relative percentage of sandstone and mudstone varies vertically and laterally within the accretionary bars. Generally, the sand grain size and proportion decrease in the downdip portion. Occasionally, the aggradational heterolithic fills occur beside the IHS. Locally in the Long Nab foreshore and Scarborough South Bay cliff section, there are packages of IHS which occur adjacent to concave cut-banks. These are more shallowly dipping than the typical IHS.

Most of the studied heterolithic deposits are concave-upward, erosionally based and locally overlain by a thin, coarse sandstone layer, and exhibit an overall fining upward trend. The individual IHS bars are up to 4 m thick and more than 100 m wide. They are sigmoidal in shape, and vertically and laterally stacked with other IHS accretion bars. In the studied sections, the sandstone strata are 10–40 cm thick alternated by 5–10 cm thick mudstone strata.

These IHS were also deposited in point bars in sinuous meandering streams. Alternation of mudstone and sandstone reflect a rhythmic variation in the hydrodynamic conditions during deposition. The presence of mud drapes, alternating sandstone and mudstone layers, abundant bioturbation and salt-water microfossils suggest proximity to a palaeoshoreline and a degree of tidal influence in sedimentation (Fisher and Hancock 1985; Wood 1985; Wood *et al.* 1988). The lower angled bar on the concave side of the channel may represent counter-point bars which form at the downstream tails of conventional bar forms in slightly confined and translating point bars (Alexander 1992*b*; Smith *et al.* 2009).

Facies association 3 (FA3): mudstone-dominated channel deposits

Facies association (FA3) is composed of planar laminated mudstones which are superficially similar to the overbank associated FA6. FA3 occur within channel-shaped scours and are commonly associated with FA1 or FA2 (Fig. 8a). They exhibit a weakly developed fining-upward trend from a siltstone-dominated lower part to an organic-rich, claystone-dominated upper part. Bioturbation is not observed, but abundant millimetre-scale lignite/coal fragments are present. They are relatively small in size: 2–4 m thick and 30–40 m wide.

The geometry and composition of FA3 suggest deposition from suspension within channel-shaped depressions. These are interpreted as the fill of channels which are abandoned during avulsion (Smith *et al.* 1989; Alexander 1992*a*; Bridge 2006; Nichols 2009). Where present, the fining-upward sequence suggests a gradual rather than a sudden avulsion (Alexander 1992*a*). In the absence of a lateral context (i.e. a cliff section), these mud plugs are difficult to distinguish from regular overbank deposits although they are commonly more organic-rich, suggesting standing bodies of stagnant water. Where the geometry can be observed they provide dimensions of the parent channels (Li and Bhattacharya 2014).

Overbank deposits

Overbank sediments constitute the dominant proportion of most of the fluvial successions exposed in Yorkshire coastal sections. The overbank successions mostly consist of mudstone, fine-grained sandstone and mud-dominated heterolithic deposits. The sandstones typically occur in crevasse splays and crevasse channels (FA4), and levee deposits (FA5). Overbank mudstones are composed of grey to dark grey mudstones with abundant organic matter and lighter grey mudstones occasionally with root traces (FA6). The pedogenically modified mudstones and sandstones are discussed within FA7.

Facies association 4 (FA4): splay sheet and crevasse channel sandstone deposits

Sharp-based, thin sand sheets and associated small ribbon-shaped sandstone deposits are common elements in the overbank of the fluvio-deltaic successions of the Ravenscar Group. Facies association 4 (FA4) is comprised of splay sheet deposits (facies association 4A) and crevasse channel deposits (facies association 4B).

Facies association 4A (FA4A): splay sheet deposits

Sheets are typically up to 2 m thick but may be up to 6 m in extreme cases. They are composed of very fine to fine-grained, current-rippled cross- and planar-parallel-stratified (occasionally structureless), sharp-based, rooted sandstone (Fig. 8b, c and e). The larger sheets are comprised of a series of beds which represent individual events. They are sharp-based and show an upward gradation from massive to planar bedding to current ripples. These sandstone beds are commonly interbedded with thin finer grained facies and palaeosols. The top surface of the sheets is commonly rooted, suggesting subaerial exposure.

Splay sheets commonly occur as isolated bodies within FA6/FA7 or occasionally they are associated with major channel deposits (FA1 and FA2). The thickness, grain size and flow energy reflected from the sedimentary structures within the sheets decrease away from the channel, i.e. from the proximal to distal part. In the proximal part, several 30–60 cm thick sandstone beds are amalgamated to form a splay body. From the medial to distal part, the grain size decreases progressively, and individual sandstone beds are separated by 5–12 cm thick, silty, very fine sandstones or mudstones (Appendix D).

The sandstone sheets are interpreted as crevasse splay deposits. Each sandstone bed within the sheet represents a single flooding event. The tractional sedimentary structures dominated laterally extensive sand sheets in the overbank are interpreted as rapid deposition from the unconfined flow during overbank flooding (Burns et al. 2017; Gulliford et al. 2017). Upward gradation of large sheets from massive to planar bedding to current ripples suggest waning of flow strength (Steel and Aasheim 1977), followed by the deposition of the suspended particles from the standing flood water. Rooting of the beds suggests that the individual flows are intermittent, and more extensive pedogenesis at the top of the sheet represents plant colonization after abandonment. Sheets are arranged into a variety of genetically related architectural elements that are discussed in the architecture section below.

Facies association 4B (FA4B): crevasse channel deposits

The small ribbon deposits have a concave shape and are up to 3 m thick but typically less than 2 m. They are erosive-based and flanked on either side by splay sheets (FA4A). They are comprised of fine- to medium-grained tabular, trough and ripple cross-stratified sandstones. Similar to FA4A, they are commonly associated with FA6/FA7 or occasionally with FA1/FA2.

The erosive-based, ribbon-shaped sandstone deposits flanked with splay sheets are interpreted as crevasse channels that fed the crevasse splays. The erosive base and concave-up shape of these overbank ribbon-shaped sandbodies suggest deposition from the turbulent and confined flows by scour and fill processes after flood breach of the parent channel (Fielding 1986; Bristow et al. 1999; Nichols and Fisher 2007; Burns et al. 2017; Lepre 2017).

Facies association 5 (FA5): mudstone-dominated heterolithic levee deposits

Facies association 5 (FA5) is composed of alternating very fine silty sandstones and mudstones (Fig. 8d). The thin silty sandstone layers show current ripple and planar-parallel stratification while the alternating mudstone layers contain parallel laminations with occasional deformation structures. Occasionally, wave-ripple lamination, planar lamination, and bioturbation are also observed. Deposits are up to a few metres thick and occur in laterally restricted bodies. They border the channel deposits and are gently inclined, thinning away from the channel body. The grain size also decreases away from the channel body.

The wedge-shaped geometry, mud-dominated heterolithic composition, unidirectional small-scale sedimentary structure and occurrence adjacent to the channel deposits suggest that these are levee deposits. They form as a result of successive small-scale overbank spilling of the channel without the development of crevasse splays (Elliott 1974; Bridge 1984). Local occurrence of symmetrical ripples and alternating dark grey mudstone suggest that they may have been deposited in a subaqueous setting.

Facies association 6 (FA6): overbank mudstone deposits

FA6 is comprised of grey and dark grey to black coloured mudstone and sporadic very fine-grained sandstone lamina (Fig. 8e, f). The mudstones are poorly planar-parallel laminated or structureless and bioturbated (BI = 2–3). Subordinate small calcareous nodules and minor desiccation cracks are occasionally present. Individual mudstone layers are 0.5–3 m thick and laterally persistent. Often they are dark in colour and contain abundant organic matter with occasional very thin laterally restricted coal layers (Fig. 8e). The light grey coloured mudstones contain less organic matter (Fig. 8f).

The freshwater bivalve *Unio kendalli* was observed within the lower part of the Saltwick Formation, 3 m above the formation base, 4 km south of Whitby (Hemingway 1974). At Hayburn Wyke, several marine microplankton were observed by Fisher and Hancock (1985) in the mudstones of the Saltwick Formation. Abundant *Unio hamatus* and *Unio distortus* occur with the Scalby Formation floodplain near Scarborough, Gristhorpe and Burniston (Hemingway 1974).

Laterally persistent, massive to planar-parallel laminated, thinly bedded mudstone suggests an overbank origin. Deposition in subaqueous conditions such as shallow-water lakes or floodplain ponds is supported by the dark grey to black colour, plane-parallel lamination, organic-rich mudstone with sporadic very fine-grained sandstone lamina, bioturbation and fossil assemblages. The light grey massive to poorly laminated mudstone with very little organic matter content and rootlets at the bed top is indicative of subaerial overbank deposition. The calcareous nodule, bioturbation and rootlets indicate pedogenic modification after deposition. Freshwater to brackish fauna suggest a minor marine influence in the southern part of the section.

Facies association 7 (FA7): palaeosol

Facies association 7 (FA7) is comprised of grey to dark grey and black mudstone to fine sandstone. This facies association is allied with FA1, FA2 or FA4 which it typically overprints. Deposits are characterized by abundant rootlets (Fig. 8c), siderite nodules and siderite spheruliths. There are also locally organic-rich horizons, nodules, bioturbation and colour mottling (Fig. 8g). The degree of modification from the original facies is varied. Examples such as those at the base of the Saltwick Formation are very well developed and 'mature' with the vertical grain-size trend, while those in the upper part of Saltwick and Scalby formations are less well developed (Fig. 8h).

Based on the presence of pedogenic features such as abundant roots, colour mottling, blocky texture and spherosiderites, this facies association is interpreted as a palaeosol. The presence of palaeosols was also described by Kantorowicz (1990) in the Long Nab Member at Burniston Bay, Alexander and Gawthorpe (1993) in the Salwick Formation at Whitby West Cliff and Rawson and Wright (1992) in both the Scalby and Saltwick formations. Two types of palaeosol are defined based upon the degree of paedogenesis: (i) comparatively mature palaeosols and (ii) poorly developed palaeosols. The former are characterized by the presence of abundant rootlets and extensive pedogenic modification. The latter are a darker grey and have sparse rootlets, and abundant carbonaceous material indicating their waterlogged origin. Livera

(1981) suggested the immature palaeosols formed in waterlogged swamps. The observed palaeosols are limited and sporadic in nature, which suggests the exposed palaeosols may be the erosional remnants of more extensive floodplain deposits (Alexander and Gawthorpe 1993).

Sandstone body architecture

A total of 83 channel bodies, 191 splay bodies and eight crevasse-channel bodies were identified and studied. Sandbody widths range from 15 to 2038 m and the thickness measured both in the field and in virtual outcrop ranges from 0.5 to 28 m with W/T ratio 15–>541 (Fig. 9). Sandbody geometry, dimension and proportions change within and between formations. Sandbodies are broadly divided into channel sandbodies consist of FA1 and FA2, and overbank sandbodies consist of FA4 and FA5.

Channel-belt facies architecture

Channel bodies are typically subdivided based on their internal stacking patterns and/or their aspect ratio. Stacking patterns include single-storey, multi-storey and multilateral (Gibling 2006; Owen *et al.* 2017). Single-storey channel bodies are deposits with no internal storey surfaces in which the thickness of the deposit equates to the depth of the channel at the time of deposition (minus compactional effects) (Friend *et al.* 1979; Hirst 1991). Multi-storey

bodies are vertically stacked channel bodies where multiple storeys are separated by erosional storey surfaces (Potter 1967). Multilateral bodies are formed by the lateral coalescence of several channel bodies representing the lateral migration of the fluvial system (Rittersbacher *et al.* 2014). The aspect ratio typically separates ribbons (W/T: <15) from sheets (W/T: >15).

We adopted and modified terminologies from the classification scheme of Hirst (1991) and Owen *et al.* (2017), and defined five different types of channel body: (i) single-storey small ribbon (W/T: 5–10); (ii) single-storey broad ribbon (W/T: 10–<15); (iii) tabular multilateral sheet (W/T: >15–30); (iv) internally stacked multi-storey sheet (W/T: 20 – >100); (v) partially amalgamated multi-storey sheet (W/T: >15–>102) (Fig. 10).

(i) Single-storey small ribbon channel bodies are isolated channel deposits with no internal storey surfaces. The channel bodies are comprised of FA1, FA2 and FA3. They represent the simplest classic channel geometry and the smallest channel dimensions (Fig. 10a-i and b-i). Thicknesses vary from 4–5.5 m and width from 25–40 m with W/T 5–10.

(ii) Single-storey broad ribbon channel bodies are larger than the single-storey small ribbon. They are 30–70 m wide and 3–5.5 m thick with W/T 10–<15. They are comprised of either single bar (FA1 and FA2; Fig. 10a-iia and b-iia) with abandoned mud fill (FA3) or multiple accretion bars formed by laterally migrated single-storey channel (Fig. 10a-iib and b-iib) followed by either aggradational fills of FA1 or FA3.
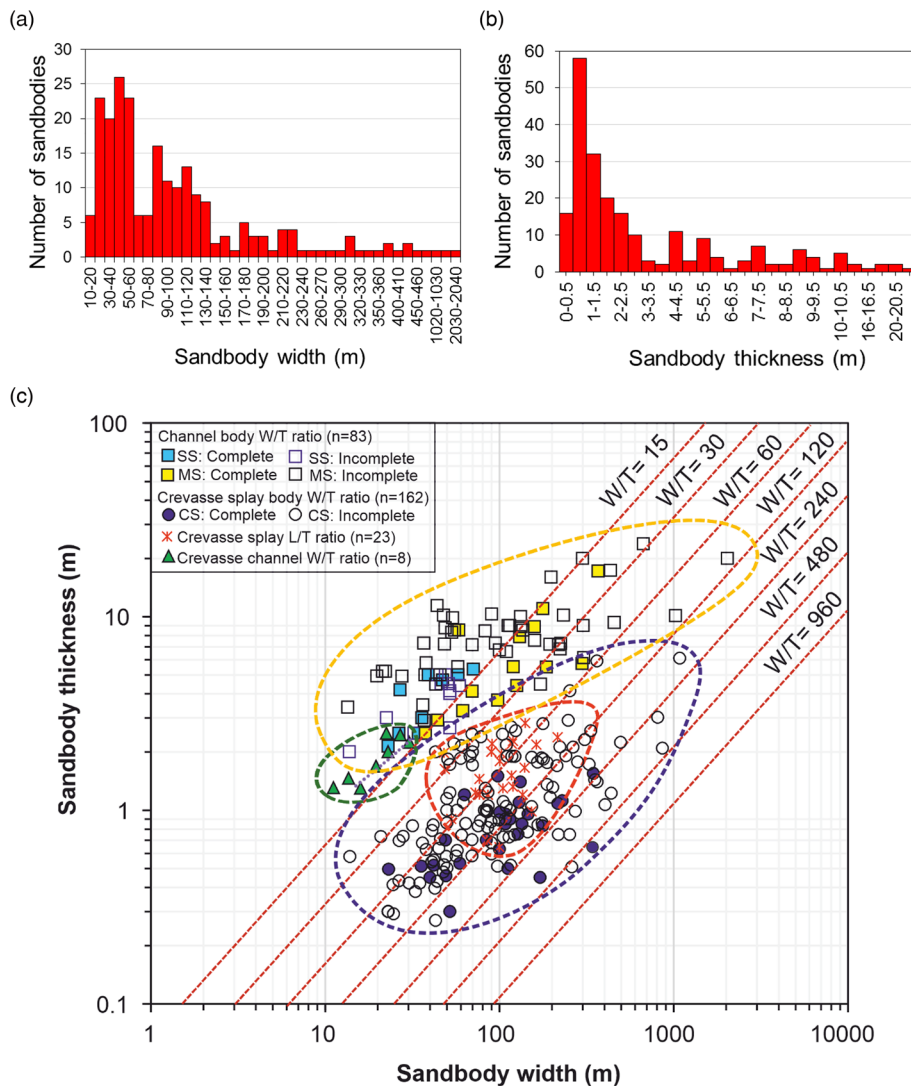

Fig. 9. Histograms and cross-plot of sandbody dimensions. (**a**) Distribution of sandbody width (both channelized and overbank sandbodies); (**b**) distribution of sandbody thickness; (**c**) cross-plot of W/T or L/T (in the case of crevasse splay) of various types of sandbodies.

(iii) Laterally stacked channel deposits consist of tabular multilateral sheet sandbodies and are bounded by flat-lying erosional basal surfaces and flat tops (Fig. 10a-iii). They are 180–> 300 m wide and 5–10 m thick with W/T up to 30. They may be filled with either inclined heterolithic strata (IHS, FA2) or accretion bars and aggradational fill of FA1. This channel type is observed in cliff sections of the Saltwick and Scalby formations. In the Saltwick Formation, several multilateral channel bodies were observed just above the Dogger Formation. The well-exposed 9 m thick and >135 m wide channel body $c.$ 2.5 km SE of High Whitby provides a good example of this type of lateral stacking pattern in cross-section (Fig. 10b-iii). The exhumed meander belt deposits of the Scalby Formation exposed between Long Nab and Scalby are excellent examples of this type of channel architecture in plan-view

(Alexander 1992b). Ielpi and Ghinassi (2014) interpreted these foreshore outcrops to represent two vertically stacked multilateral channel bodies.

(iv) Internally stacked multi-storey sheets have a simple external geometry like multilateral channel bodies, but the internal stacking pattern is more complex. Both the multi-storey and multilaterally stacked channel deposits overlie a single major basal surface (Fig. 10a-iv).

Channel bodies are 600–>1000 m wide and 9–20 m thick with a W/T ratio up to 100. They consist of both laterally and vertically stacked deposits of FA1 with occasional FA2 and FA3. Channel bodies typically comprise 3–4 stacked storeys in the vertical section and the storeys are 130–415 m (observed width) wide and 2.5–7.3 m thick. The original storey widths and thicknesses may have
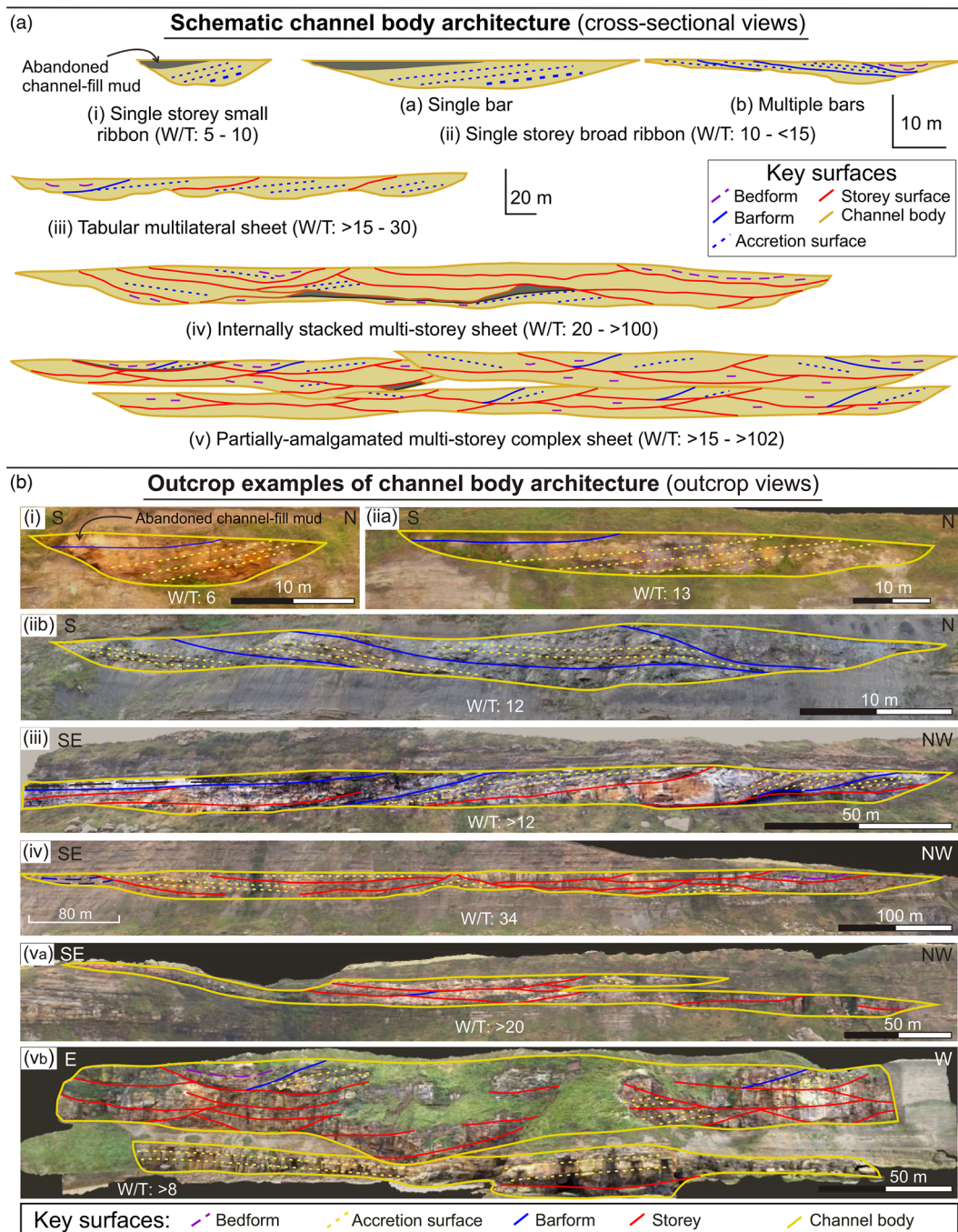

Fig. 10. Schematic channel sandbody architecture (**a**) and outcrop examples of architecture (**b**) including: (i) single-storey small ribbon; (ii) single-storey broad ribbon with (**a**) single bar and (**b**) multiple bars; (iii) tabular multilateral sheet; (iv) internally stacked multi-storey sheet; (v) partially amalgamated multi-storey sheet complex (including va and vb).

been greater but are eroded by younger channels that truncate the older channel storey. The channel deposits of the Saltwick Formation exposed at the High Whitby section are an example of the internally amalgamated multi-storey sheet (Fig. 10b-iv). Mjøs and Prestholm (1993) interpreted this channel as a multi-storey channel body with complex and long-lived history. The Moor Grit channel bodies at Hundle Point and the Scarborough South Bay sections are also a good example. These channels were interpreted by Alexander and Gawthorpe (1993) as complex multilateral sheets but are reclassified here based on the mapped storey surface pattern and major incisional basal surfaces.

(v) Partially amalgamated multi-storey sheet complexes are channel complexes where vertically and laterally stacked channel bodies are partially connected (Fig. 10a-v) with pockets of floodplain mudstones in between the sheets. This channel body geometry is generally comprised of FA1, FA2 and FA3. The channel bodies are very thick and wide; thickness ranges from 16 to 28 m and width from >312 to >2038 m with W/T up to >102. A combination of multi-storey and multilateral storey patterns are observed. Within individual channel bodies, stories are both amalgamated and may cross-cut one another. Individual storeys are 100–>190 m wide (observed width) and 2.5–8.2 m thick.

Channel bodies at Beacon Hill Cliff (Fig. 10b-va), Whitby West Cliff (Fig. 10b-vb) and Kettleness in the Saltwick Formation, and at Ravenscar in the Sycarham Member of the Cloughton Formation are examples of this type. The multi-storey offset channel deposits (type-3bi) and stacked sandbody with no obvious offset migration (type-3bii) of Alexander and Gawthorpe (1993), and the amalgamated complex of Hirst (1991) are similar to the partially amalgamated multi-storey sheet complex geometry. In partially amalgamated channel bodies, it is difficult to discern the individual channel/channel body. This feature along with the existence of pocket floodplain deposits suggests that the aggradation rate was comparatively low and the younger channels or channel bodies incised into the older channel bodies.

Overbank facies architecture

Crevasse channels and splays (FA4) are the major overbank constituents in all of the formations. A total of five types of sandbody architectures were observed in the overbank settings: (i) ribbon crevasse channel, (ii) single-splay sheet, (iii) amalgamated splay sheet, (iv) splay sheet complex and (v) wedge levee deposits (Fig. 11).

(i) The crevasse channel bodies are composed of ribbon sandstones of FA4. They are commonly 1.5–2.5 m (average 2 m) thick and 10–25 m (average 20 m) wide with W/T ratio less than 11 (Fig. 11a-i and b-i). They have an erosive base and cut into overbank mudstone, especially in the proximal or proximal medial part of the splay. They are interpreted to represent the channels that fed the splay deposits during flood events.

(ii) Single crevasse splays consist of FA4. They are small-scale, 0.3–2.2 m (average 1 m) thick and >20–300 m (80 m) wide with W/T ratio >20–540 (average 95). They are lenticular or sheet-like sandbodies encased in overbank mudstone or bounded by palaeosols (Fig. 11a-ii and b-ii). They are interpreted to form as a result of overbank flooding and sediment deposition during excess discharge of single or multiple events through a single breach point in the channel. The lack of internal palaeosols or rooting suggests these features are relatively short-lived.

(iii) Coalesced moderate- to large-scale elongated (parallel to the feeder channel) crevasse splay sandbodies are termed amalgamated splays. These can be subdivided into three different types based upon the stacking of the constituent splays. They may

be vertically amalgamated, laterally amalgamated, and both laterally and vertically amalgamated (Fig. 11a-iii and b-iii). Vertically amalgamated splays are formed by an amalgamation of two generations of splay where >50% of the younger splay base is in contact with an older splay. Vertically stacked splays are >35–780 m (average 320 m) wide, 140 m long and 0.6–3.8 m (average 2 m) thick with W/T ratio >15–265 (average 85). They are recognized by sharp/erosional contact or rooted horizons between the splay bodies along with more than one coarsening or fining-upward trend (Fig. 11a-iiia and b-iiia). They are generally thicker than the single and laterally amalgamated splay body. Laterally amalgamated splays are elongated; connected splay sheets form parallel to the feeder channel where splay-to-splay contacts are <50% (Fig. 11a-iiib and b-iiib). They are >70–930 m (average 270 m) wide, 0.53–2.2 m thick with W/T ratio 85–600 (average 200). They are generally larger than the single crevasse splays, and in cross-section, they have a lensoid geometry.

Laterally and vertically amalgamated splay bodies are stacked splay bodies where splay bodies are connected laterally and vertically separated by pockets of floodplain deposits. They are >50 to 1170 m wide, 2.5–5.8 m thick with W/T ratio >30–275 (average 150) (Fig. 11a-iiic and b-iiic). This type of splay body is interpreted to be deposited by aggrading sinuous feeder channels from multiple input points.

(iv) Splay complexes are large-scale >1285 m wide (length and width up to several km; 20 km described by Mjøs, *et al.* 1993), up to 6.5 m thick with W/T ratio >240. They comprise several upward-coarsening packages and crevasse channel deposits (FA4) (Fig. 11a-iv and b-iv). Sandstone bedsets are separated by thin, bioturbated to plane-parallel laminated mudstone. Splay complexes were observed in the Gristhorpe Member at Cloughton Wyke and Ravenscar. At Cloughton Wyke, clear tidal indicators such as plane-parallel stratified sandstone with double mud drapes, flaser, wavy and lenticular beddings were observed. Sedimentary structures along with palynofacies analysis of Hancock and Fisher (1981) indicate the marine influence and deposion in a tidal influenced delta plain.

(v) Natural levees are wedge-shaped, laterally restricted, gently inclined, channel-associated bodies (Fig. 11a-v and b-v). They are rarely observed, 30–50 m wide and 2–3 m thick with W/T ratio *c.* 20. Levees are entirely composed of FA5. They are thicker in the channel proximal part and gradually taper away from the parent channel.

The studied facies associations and sandbody architectural patterns indicate that the non-marine successions of the Ravenscar Group were deposited in a fluvio-deltaic depositional condition (Fig. 12) dominated by highly sinuous channel deposits.

Temporal variations in facies and sandbody architectures

Facies and sandbody architectures vary widely within and between the formations. VO data provide an opportunity to map facies variations and trends in the fluvial stacking patterns and architecture. In this study, we adopted the methodology of Rittersbacher *et al.* (2014) for looking at lateral and vertical trends in facies associations and channel body dimensions from VO data. Individual channel bodies were identified, mapped and quantified. Their vertical position relative to a stratigraphic datum was recorded along with the proportion of channels in a section. Their lateral position in a depositional dip profile and with respect to the major structures was also noted. Lateral and vertical trends were studied over a 40 km long, oblique (7°–45° except Whitby West Cliff where it is 90°) depositional dip section from Kettleness in the NW to Scarborough South Bay in the SE (Fig. 13). The detailed vertical variations of channel body width, thickness and cross-sectional area
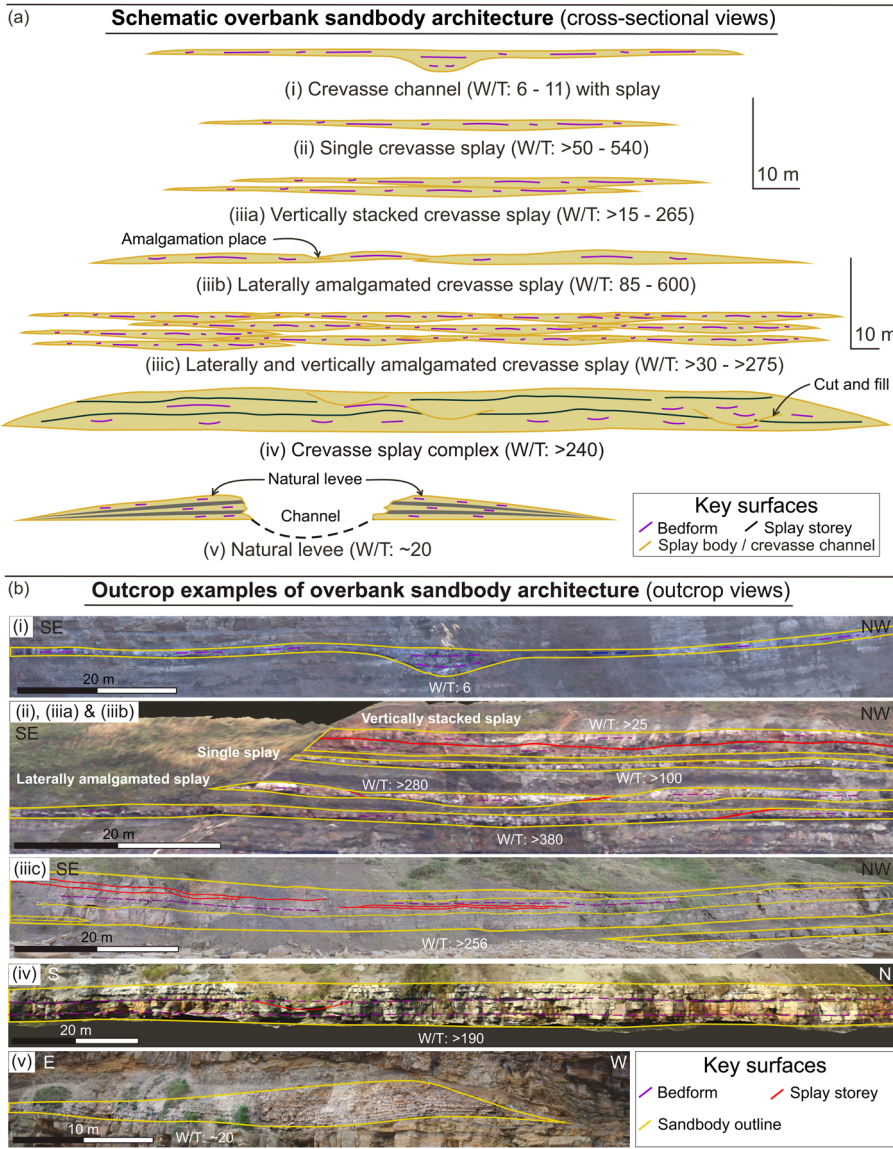
Fig. 11. Schematic overbank sandbody architecture (**a**) and outcrop examples of architecture (**b**) including: (i) crevasse channel, (ii) single crevasse splay, (iiia) vertically stacked crevasse splay, (iiib) laterally amalgamated crevasse splay, (iiic) both laterally and vertically amalgamated crevasse splay, (iv) crevasse splay complex and (v) natural levee.
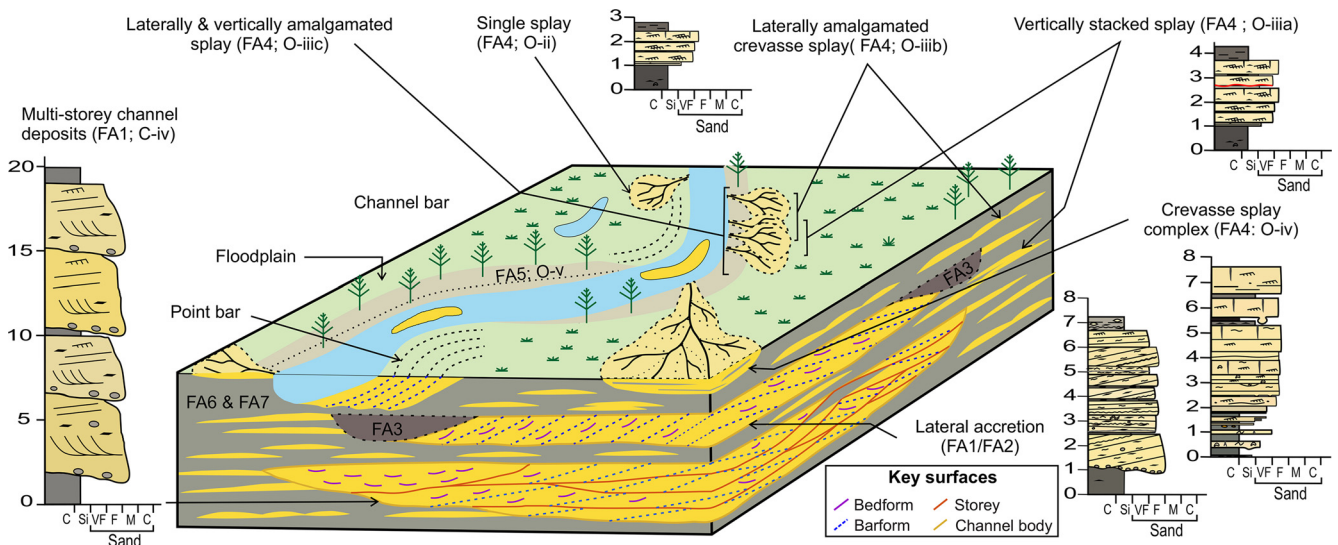

Fig. 12. Schematic block diagram showing examples of the distribution of different facies associations (FA1–FA7) and sandbody architectures (C: channel body and O: overbank) in the fluvio-deltaic successions of the Ravenscar Group.
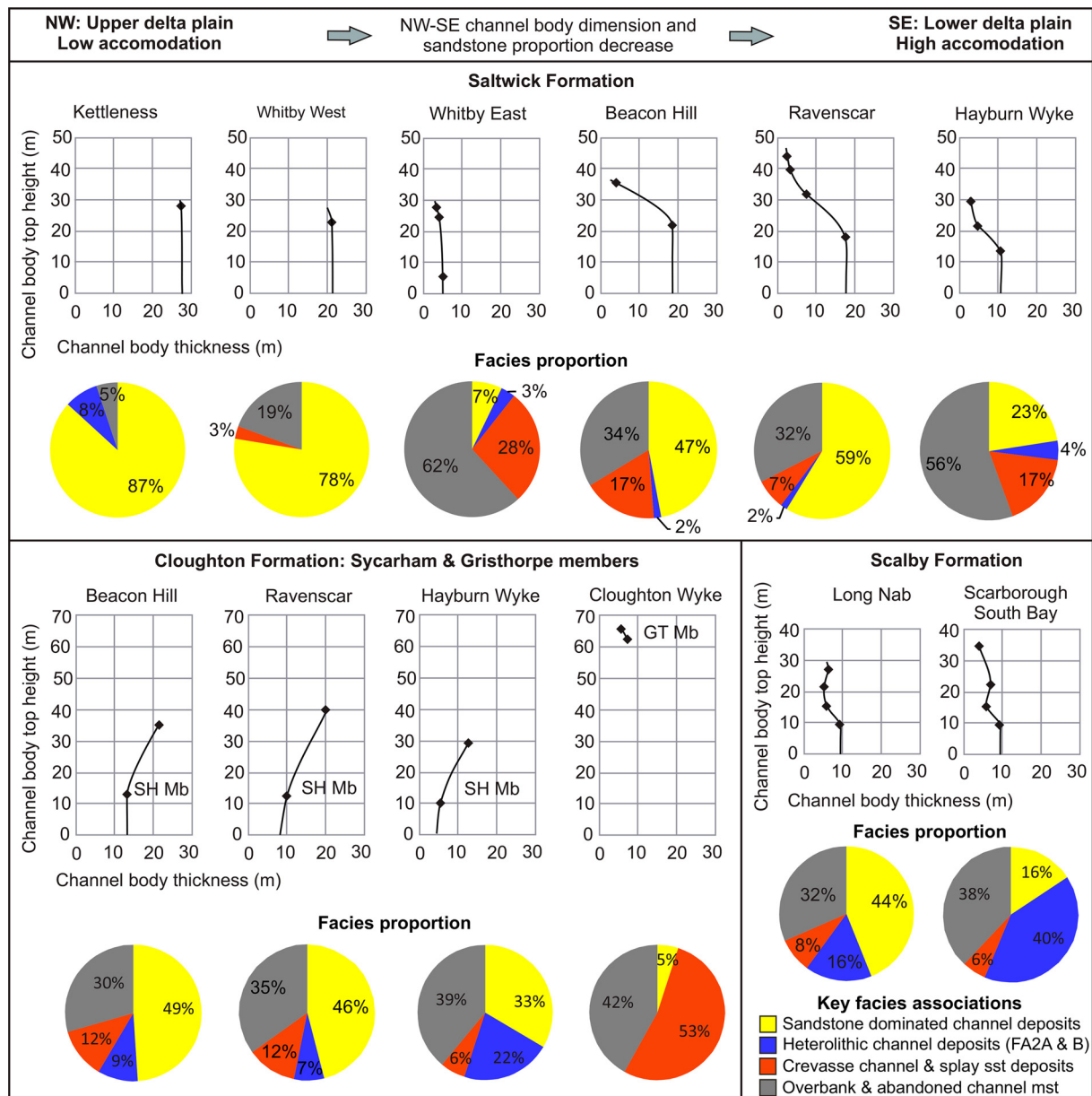
Fig. 13. Spatial variation of channel body dimension and coarse-grained facies proportion. Channel body dimension and facies proportion decrease from the northwestern to southeastern part of the exposures. A similar decreasing trend is observed in all the studied fluvio-deltaic formations.

were studied by plotting these parameters against their stratigraphic height measured from the top of the Dogger Formation (Fig. 14). These data were binned into 10 m thick packages to remove local lateral variations intrinsic to channel bodies. The majority of the channel bodies are between 50–500 m wide and 3–12 m thick (Fig. 14a, b). In the following sections the facies, facies associations and architecture along with their lateral and vertical variations in the fluvio-deltaic formations that make up the Ravenscar Group are systematically described.

Facies architecture of the Saltwick Formation

The Saltwick Formation was studied at six outcrops along 14.5 km of very steep coastal cliffs (Appendix E). The base of the formation is marked by an erosional unconformity on top of the marine sandstone deposits of the Dogger Formation or locally the Whitby Mudstone Formation (at Kettleness; Appendix E). The top of the formation is a marine flooding surface at the base of the shallow marine Eller Beck Formation. The Saltwick Formation varies in thickness from 28 to 45 m.

Ten field-based sedimentary logs and 96 virtual logs were used to study the facies proportion. All the facies associations (FA1–FA7) were observed in this formation. The proportion of coarse-grained facies (FA1, FA2, and FA4) in the formation ranges from 38–95% (avg. 65.7%) and the mudstone facies proportions range from 5–62% (average 34.3%) (Fig. 15). At the Kettleness, Whitby West, and in most parts of the Beacon Hill and Ravenscar sections, the Saltwick Formation is dominated by FA1 (up to 95%; Fig. 15). At the Whitby East and locally at the Beacon Hill sections it is dominated by FA6 (up to 75%) and FA4 (up to 28%) (Fig. 15).

A total of 41 channel bodies and 134 crevasse splay bodies were identified and studied. The corrected dimensional properties of the sandbodies are given in Table 3 and Figure 16. Most of the channel bodies are multi-storey and multilateral ($n = 34$) and show partially amalgamated, internally stacked and tabular multilateral geometries. They are >30–2038 m wide and 5–20 m (average 8 m) thick (Fig. 16). There are fewer single-storey channel bodies ($n = 7$) which are composed of FA1–FA3. They show both the small and broad ribbon geometries (Fig. 16). The width of the channel bodies ranges from 42–62 m (average 50 m) and thickness from 3–3.5 m
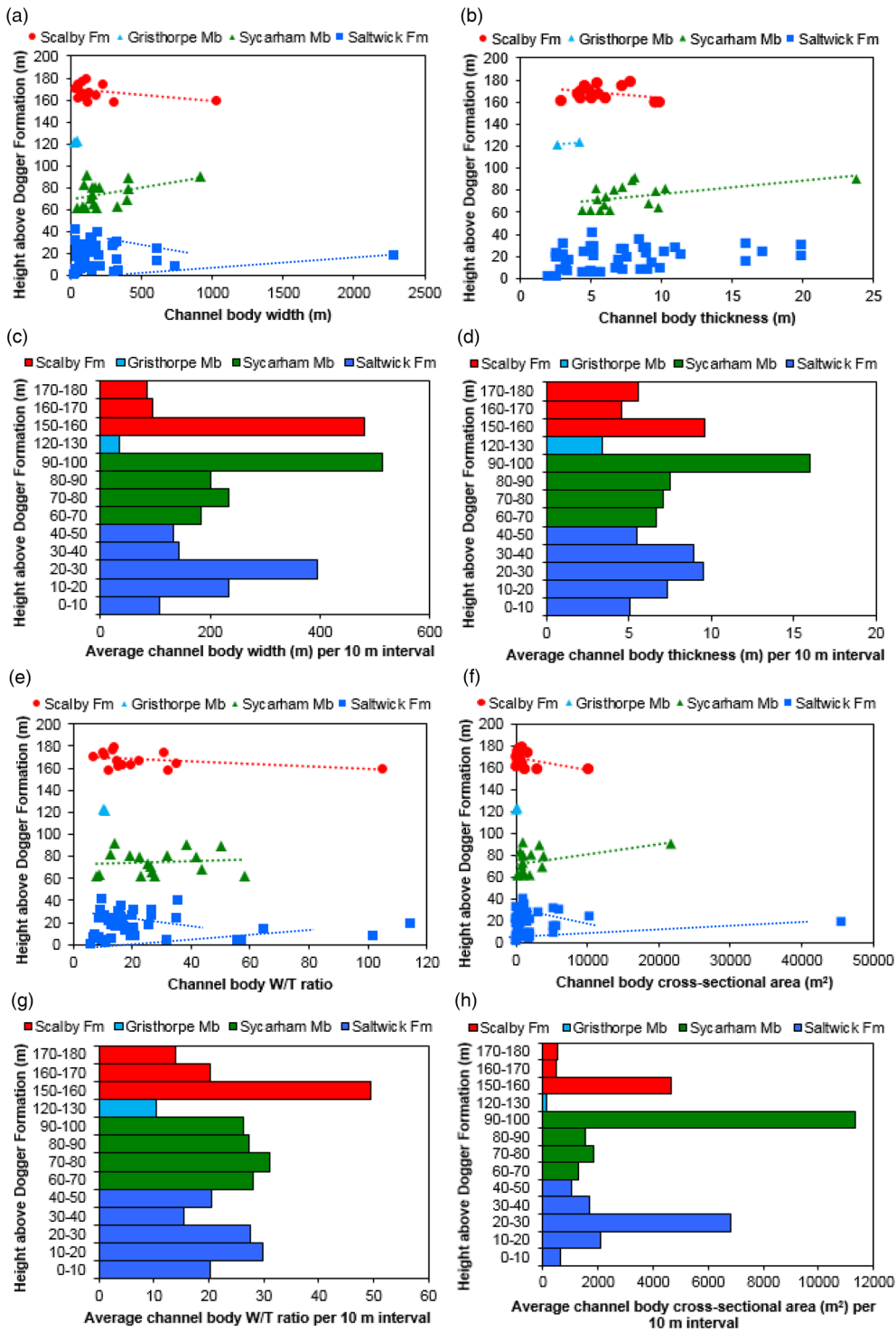
Fig. 14. Cross-plots of channel body (**a**) width and (**b**) thickness plotted against their stratigraphic position. Histograms of channel body (**c**) width and (**d**) thickness averaged over 10 m intervals and plotted against their stratigraphic height above the Dogger Formation. Cross-plot of channel body (**e**) *W/T* and (**f**) cross-sectional area against stratigraphic height. Histogram of channel body (**g**) *W/T* ratio and (**h**) cross-sectional area against stratigraphic height averaged over 10 m intervals.

(average 3.5 m) (Fig. 16). Crevasse splay bodies consist of the single and amalgamated splay bodies (overbank architectural type-ii and type-iii). Single crevasse splay bodies are less extensive and show lower *W/T* ratio than the amalgamated splay bodies (Table 3; Fig. 17).

In the Saltwick Formation, the channel body maximum thickness decreases from 28 m in the Kettleness outcrop in the NW of the study area to 11 m in the Hayburn Wyke outcrop in the SE of the area. The resultant coarse-grained facies proportion decreases from 95 to 38% towards the SE (Fig. 13). Within this regional trend, there are some local variations. The Kettleness, Whitby West and Ravenscar (east of Peak Fault) outcrops are dominated by multi-storey channel-fill deposits whereas the Whitby East and Ravenscar Quarry Cliff sections (west of the Peak Fault) are dominated by overbank mud and crevasse splay deposits with a few small-channel bodies. Both channel and overbank dominated parts are present in the Beacon Hill Cliff section (Appendix E). Figure 18 is a 22 km long cross-section which includes 46 virtual logs to illustrate the lateral architectural and facies variations. These new data indicate that some thick multi-storey channel bodies are fault-bounded (at the Whitby West and Ravenscar sections) and others are not (at the Kettleness and Beacon Hill (Black Nab to Widdy Head) sections). Average channel body dimensions (width and thickness) in the Saltwick Formation increase until 20–30 m stratigraphic height and then decrease in the upper part of the formation (Fig. 14c–f).

The overall thickness of the Saltwick Formation increases towards the SE from 28 m at Kettleness and Whitby East to 43 m at Ravenscar. The formation thickness varies locally around the
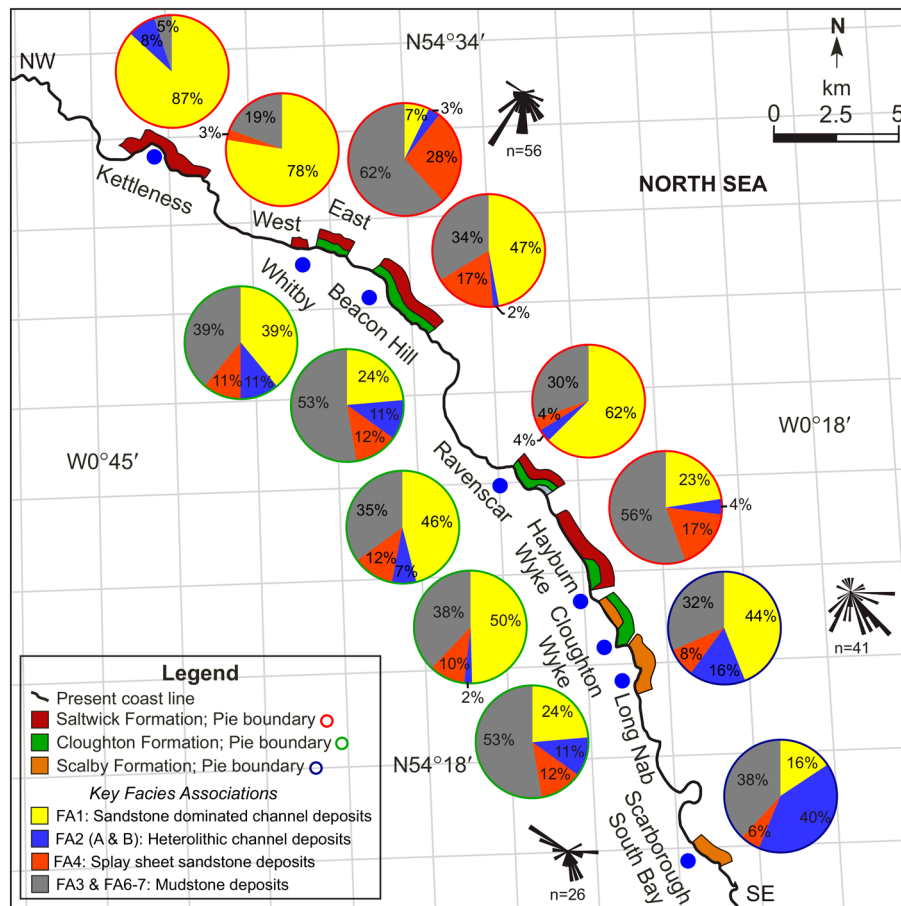
Fig. 15. Proportion of facies associations at outcrops within the study area. Pie charts with red outline are from the Saltwick Formation, green from the Cloughton Formation, and blue from the Scalby Formation.

Peak Fault in Ravenscar (Fig. 19) where the average thickness measured on the hangingwall side of the Fault is 43 m (max. 45 m due to channel scouring). In the footwall side, Pliensbachian Staithes Sandstone and Redscar Mudstone formation are juxtaposed against the Dogger and Saltwick formations on the hangingwall side (Fig. 19b, c). Over 50 m of Toarcian (Lower Jurassic) deposits of the Blea Wyke Sandstone Formation and the upper part of the Whitby Mudstone Formation are absent in the footwall section. The Eller Beck Formation is not exposed in the footwall part of the section, so the full Saltwick Formation thickness cannot be determined (Fig. 19d, e). A 1 m thick Dogger Formation is exposed at Quarry Cliff section (1 km west of Coastal Cliff exposure) in the footwall block. The formation thickness increases from 1 m in footwall to 19 m in hangingwall.

Facies architecture of the Cloughton Formation

The Cloughton Formation was studied in five outcrop sections which include 12.8 km of the cliff line. Only the lower part of the formation, i.e. part of the Sycarham Member, is exposed in the Whitby East and Beacon Hill sections. The complete formation is exposed at the Ravenscar, Hayburn Wyke and Cloughton Wyke Cliff sections although the exposures are partially covered in vegetation. The formation thickness measured in the Ravenscar section was *c.* 80 m.

Four field-based sedimentary logs and 26 virtual logs were collected to determine the facies proportion. All of the facies associations were observed in this formation. The average coarse-grained facies (FA1, FA2 and FA4) proportion ranges from 58–70% and the fine-grained facies (FA3 and FA6–7) from 30–42% (Fig. 15). In the Sycarham Member, the predominant facies constituent is FA1 (up to 59%), and in the Gristhorpe Member, the primary constituent is FA4 (up to 53%).

A total of 20 channel bodies and 21 crevasse splay bodies were identified and studied. The dimensional properties of the sandbodies are given in Table 3 and Figures 16 and 17. The majority of the channel bodies (n = 15) are multi-storey and represent partially amalgamated or internally stacked channel body architectures. They are composed of FA1–FA3, and are 25–>765 m wide and 5–24 m (average 8 m) thick (Fig. 16). All of the observed multi-storey channel bodies occurred in the Sycarham Member, and only two single-storey channel bodies were studied in the Gristhorpe Member. The single-storey channel bodies are composed of FA1 and FA2. They are 30–70 m (average 42 m) wide and 3–4.5 m (average 3.9 m) thick (Fig. 16) which show both the small and broad ribbon geometries. Three different types of splay body architectures were observed in this formation. The single-splay bodies are 46–295 m (avg. 120 m) wide, 68 m long and 0.5–2 m (average 1.1 m) thick. Laterally amalgamated splay is incomplete and >68 m wide and 1.28 m thick. The crevasse splay complexes are 175–>1285 m (avg. 645 m) wide and 3–6.5 m thick (Fig. 17).

In the Sycarham Member of the Cloughton Formation, channel body thickness decreases from *c.* 20 m in the Beacon Hill outcrop (NW) to *c.* 10 m in the Cloughton Wyke outcrop (SE; Fig. 13). The coarse-grained facies proportion also decreases from 70 to 60% in the respective sections. Average channel body dimensions (width and thickness) in the Sycarham Member of the Cloughton Formation show an upward increase (Fig. 14c–f). Channel body cross-sectional area (width × thickness) also shows a similar trend.

Facies architecture of the Scalby Formation

The Scalby Formation was studied in 4 km of coastal cliff sections at Long Nab, Scarborough South Bay, Cromer Point and the northwestern part of Cloughton Wyke. The complete vertical section of the formation is not exposed in any of the studied

Table 3. *Dimensional data of sandstone bodies in different formations of the Ravenscar Group*

Formation	Sandbody type	Width (m)			Thickness (m)			W/T		
		Min.	Avg.	Max.	Min.	Avg.	Max.	Min.	Avg.	Max.
Scalby Formation	Channel body (n = 21)	>23	-	>1026	2	6	10	6	21	>102
	Single storey (n = 7)	23	40	70	2.5	3.8	5	6	10	14.0
	Multi-storey (n = 14)	>50	-	>1000	4.5	7	10	>15	23	>100
	Crevasse splay body (n = 32)	25	125	336	0.5	1	2.5	>26	95	470
	Single splay (n = 29)	25	64	270	0.5	1	2	>25	80	225
	Amalgamated splay (n = 3)	107	250	340	0.7	1.1	2.5	107	235	470
Cloughton Formation	Channel body (n = 20)	>25	140	>764	3	7.5	24	8	20	54
	Single storey (n = 5)	30	42	70	3	4	4.5	8	11	12
	Multi-storey (n = 15)	>25	-	>765	5	8	24	>15	24	54
	Crevasse splay body (n = 20)	>46	-	>1285	0.5	1.8	6.5	>40	102	280
	Single splay (n = 16)	>46	120	295	0.5	1.1	2	40	106	280
	Amalgamated splay (n = 1)	>68	-	-	-	1.3	-	>40	-	-
	Splay complex (n = 3)	>345	715	>1285	3	5.5	6.5	>65	150	>240
Saltwick Formation	Channel body (n = 41)	>14	160	>2038	2	7.5	28	10	24	102
	Single storey (n = 7)	42	50	62	3	3.5	3.5	10	12	13
	Multi-storey (n = 34)	>30	225	2038	5	4.5	20	>15	25	102
	Crevasse splay body (n = 133)	>30	288	913	0.3	1	3.9	>20	105	541
	Single splay (n = 92)	>30	108	365	0.3	2	2.2	>20	97	541
	Amalgamated splay (n = 41)	>67	288	906	0.5	2.2	3.8	>30	120	440

Channel and crevasse splay body architecture
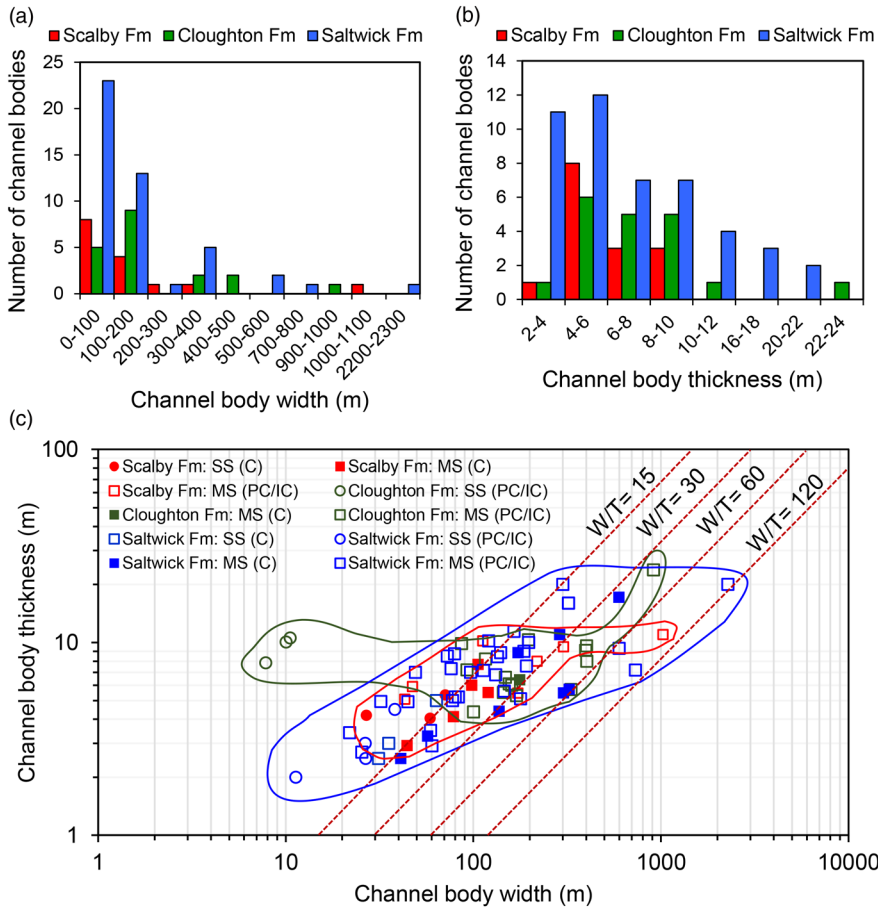
21

Fig. 16. Channel body dimensional data. Histograms of channel body width (**a**) and channel body thickness (**b**). Red, green and blue bars represent the Scalby, Cloughton and Saltwick Formations respectively. (**c**) Cross-plot of channel body *W/T*. Filled shapes represent the complete channel body (C) whereas the empty shapes represent the partially complete (PC) or incomplete (IC) channel body. SS (C): single storey (complete); MS (C): multi-storey (complete); SS (PC/IC): single storey (partially complete/incomplete); MS (PC/IC): multi-storey (partially complete/incomplete).
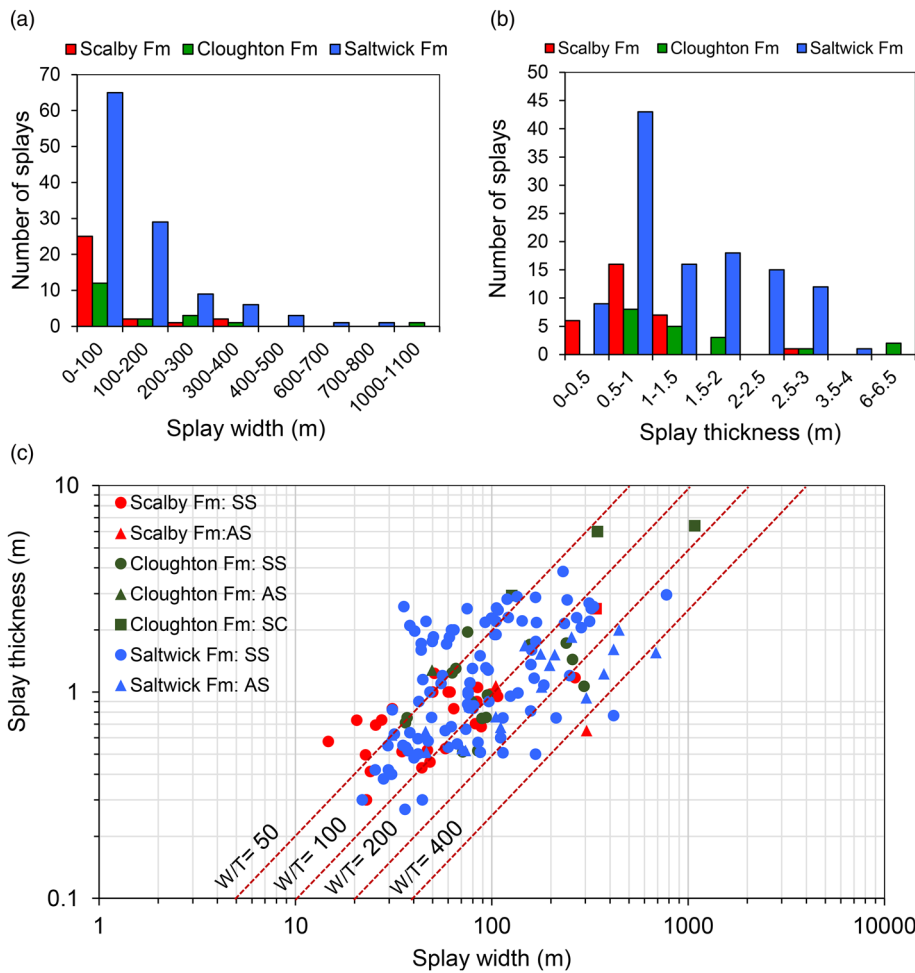

Fig. 17. Dimensional data of crevasse splays. Histograms of the splay width (**a**) and (**b**) splay thickness. Red, green and blue bars represent the Scalby, Cloughton and Saltwick Formations respectively. (**c**) Cross-plot of splay *W/T*. SS: single splay; AS: amalgamated splay; SC: splay complex.
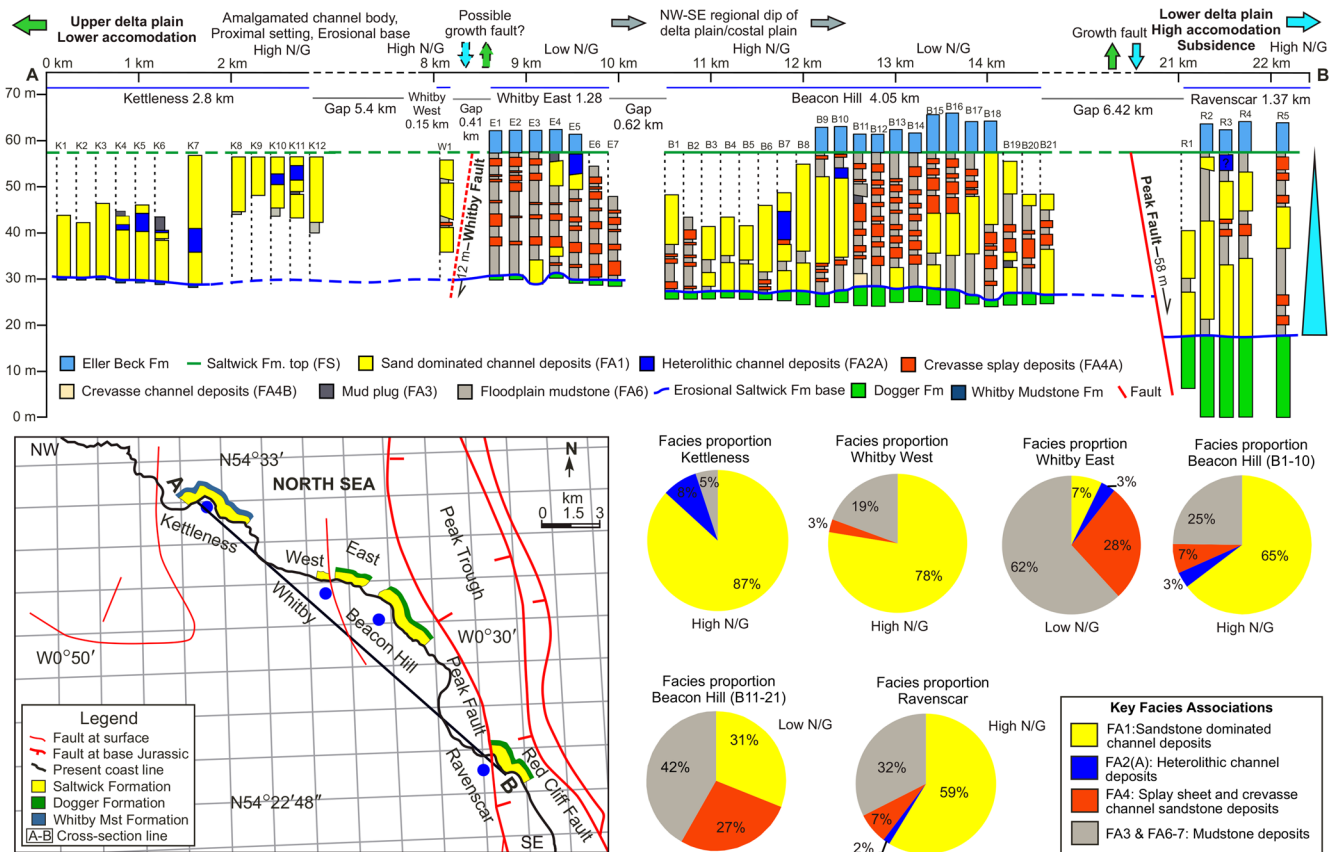
Fig. 18. Cross-section along AB, a 22 km long exposed section of the Saltwick Formation between Kettleness and Ravenscar. The blue and green lines represent the base and top of the Saltwick Formation. The pie charts show the average facies proportion in various sections.

sections. The stratigraphic thickness of these outcrops ranges from 28–40 m. The beds dip towards the south, and in the northwestern sections, the lower, sand-dominated part of the formation (Moor Grit Member) is exposed at the top of the cliff while towards the south, the Moor Grit passes into the subsurface and the cliff sections are comprised of the finer-grained Long Nab Member (Appendix E).

A total of 26 field-based sedimentary logs, 27 borehole core logs and 20 virtual logs were studied. The average coarse-grained facies (FA1, FA2 and FA4) of the formation ranges from 60–70%, while the fine-grained facies (FA3, FA6 and FA7) range from 30–40% (Fig. 15). FA1 is the predominant facies constituents (up to 46%) of the formation and FA2, and FA4 individually comprise 7–8%.

A total of 21 channel bodies and 36 crevasse splay bodies were identified and studied. Channel body widths were corrected in relation to the palaeocurrent direction of individual channel bodies (135–225°) when data were available; otherwise, the predominant palaeocurrent direction (170°) was used. The dimensional properties of sandbodies are given in Table 3 and Figures 16 and 17. The majority of the studied channel bodies (*n* = 15) are multi-storey and mainly represent internally stacked and tabular multilateral sheet architectures. They are composed of FA1 and FA2 and are 50–>1000 m wide and 4.5–10 m thick with *W*/*T* ratio 15–>100. The single-storey channel bodies are also composed of FA1 with occasionally FA2 and FA3. They were observed in the upper part of the formation, and show both the small and broad ribbon architectures (Appendix E).

Crevasse splay bodies are composed of the single and amalgamated splay bodies (overbank architectural type-ii and type-iii). The single-splay bodies are 25–336 m (average 125 m) wide, 35–>100 m long, and 0.51–1.96 m (average 1.1 m) thick. The laterally amalgamated splays are 107–>310 m wide and 0.65–2.5 m (average 1.1) thick (Table 3; Fig. 17).

No lateral trends in channel body dimensions were observed in the Scalby Formation, but an increase in the fine-grained facies proportion and the presence of IHS and other evidence for marine influence, towards the SE were seen (Fig. 13). There is a continuing upward decrease in average channel body dimensions in the Scalby Formation which is slightly interrupted between 170–180 m above datum by a comparatively thick channel body at Burniston Bay. The channel body *W*/*T* ratio and cross-sectional area (width ×thickness) also show a similar trend (Fig. 14e–h).

Discussion

The data collected during the course of this study allow a unique insight into a series of sections that have already been extensively studied (Hemingway and Knox 1973; Leeder and Nami 1979; Livera and Leeder 1981; Alexander 1992*a*, *b*; Eschard *et al.* 1992*a*; Alexander and Gawthorpe 1993; Mjøs *et al.* 1993; Mjøs and Prestholm 1993; Ielpi and Ghinassi 2014). The addition of VO data and the integration of VOs with outcrop and behind-outcrop sedimentary logs allows quantification of the deposits that has not been previously possible. These data have been used to address four issues for these sections: (i) the sequence stratigraphy, including vertical and downdip trends in fluvial stacking and architecture, (ii) the role of syn-depositional faulting in locally controlling the depositional systems, (iii) architecture of overbank sandbodies and their role in paralic reservoirs, and (iv) comparison of sandbody dimension with analogues. These aspects are discussed below.

Sequence stratigraphy and channel-stacking patterns

In this study, we recognize two unconformity bounded sequences which consist of smaller parasequences bounded by marine
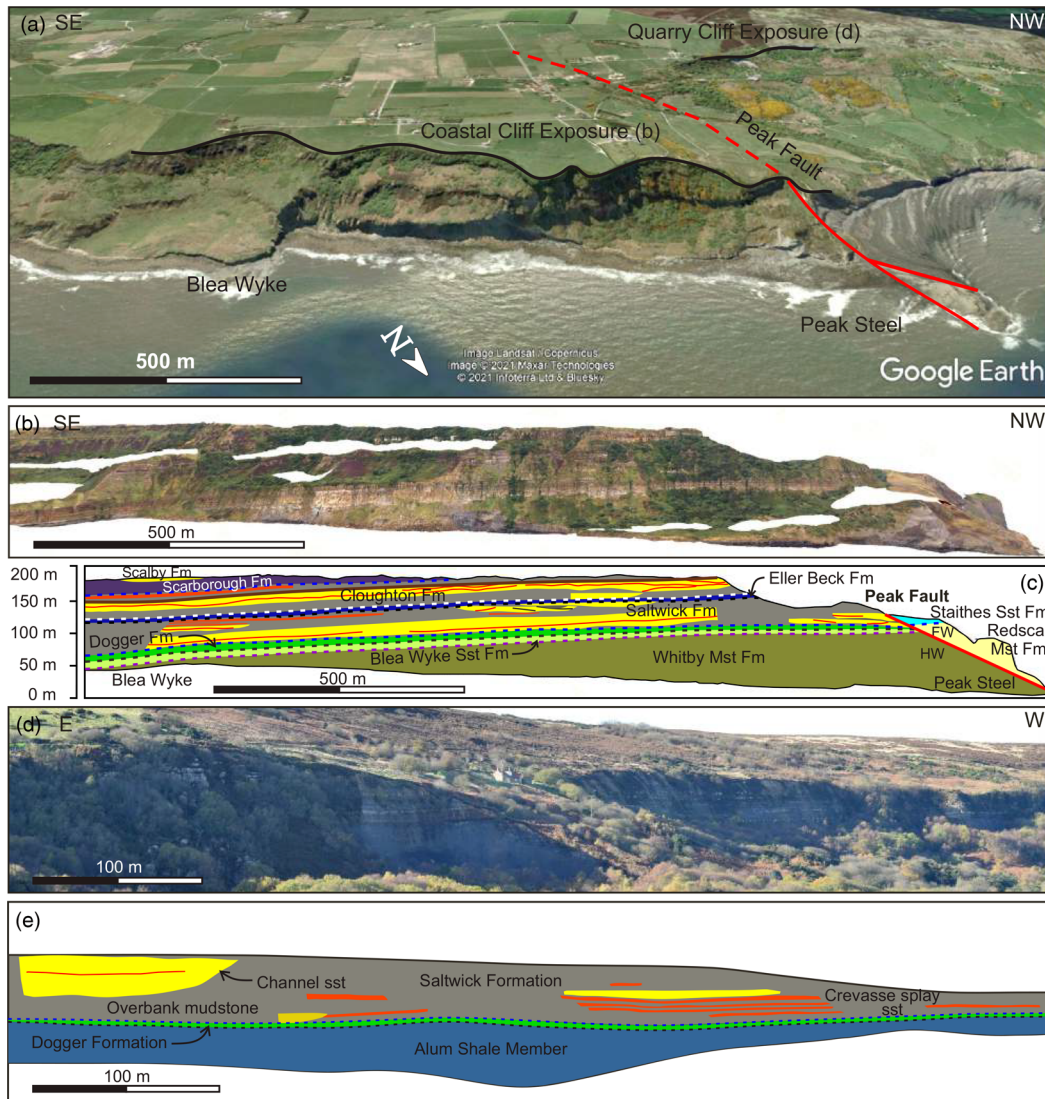
Fig. 19. Lithostratigraphic correlation panels and thickness variability across the Peak Fault. (**a**) Google Earth image taken at an eye altitude of about 1 km facing toward the cliff showing the position of the Peak Fault, coastal cliff exposure and quarry cliff exposure. (**b**) Drone-based 3D VO of the hangingwall coastal cliff section. (**c**) Detailed lithostratigraphic and facies interpretation of hangingwall coastal cliff exposure. The gully between the outcrops is the trace of the fault plane of the Peak Fault and the left side is the hangingwall block (HW) whereas the right side is the footwall block (FW). In the hangingwall side, the Saltwick Formation overlies the Dogger Formation, but in the footwall (right) side the Staithes Sandstone Formation overlies the Redscar Mudstone Formation at the same topographic level. (**d**) Photograph taken from *c.* 1 km west of the Peak Fault, at the quarry cliff exposure where the Saltwick Formation is exposed. (**e**) Detailed lithostratigraphic and facies description of the quarry cliff exposure. At this location, the Dogger Formation is 0.5–1 m thick and unconformably overlies the Alum Shale Member of the Whitby Mudstone Formation. The top of the Saltwick Formation is not preserved due to present-day erosion.

flooding surfaces. The lower sequence, termed here Sequence A, is bounded at the base by the angular Mid-Cimmerian Unconformity (Hemingway 1974; Alexander 1989; Underhill and Partington 1993) and separated from the overlying Sequence B by the Late Bajocian unconformity (Powell 2010; Fig. 4). Both the sequences are type 1 sequences of Van Wagoner *et al.* (1988). Sequence A is Aalenian to Bajocian in age, comprises the majority of the Ravenscar Group and contains five parasequences (PS 1–5; Fig. 4 and Table 4). There is an increase in the proportion of marine deposits within successive parasequences, suggesting they are part of a long-term transgressive trend. The overall decreasing channel proportion and dimensions, and increasing overbank mud proportion, also reflect the retrogradational trend (Table 4).

Sequence B unconformably overlies Sequence A and represents a return to a fluvio-deltaic setting. This sequence is comprised of the Scalby Formation. Earlier workers have ascribed a significant time gap to the unconformity at the base of the Scalby Formation (Powell

2010), although a palynological study by Riding and Wright (1989) suggested only a minor stratigraphic break. Regardless of the duration, erosively based, multi-storey amalgamated channel deposits abruptly overlie marine deposits, suggesting a major reorganization of the depositional system. Vertical trends in channel body proportions and dimensions in Sequence B also show a retrogradational stacking pattern (Table 4). The following section discusses the channel stacking patterns within the two sequences.

Fluvial stacking patterns are primarily controlled by two key factors: the accommodation to sediment supply ratio (A/S), especially with respect to fluvial base-level (Wright and Marriott 1993; Shanley and McCabe 1994; Holbrook *et al.* 2006) and the position within the depositional system, especially in distributive fluvial systems (DFSs; Hartley *et al.* 2010; Weissmann *et al.* 2010, 2013; Rittersbacher *et al.* 2014; Owen *et al.* 2015). Stacked multi-storey fluvial sandbodies such as those that occur in the lower parts of the Saltwick Formation (PS 1) and the upper part of Sycarham

Table 4. *Marine v. fluvial sedimentation in the Ravenscar Group and changing fluvial sandbody proportion and dimension between parasequences*

	Stratigraphic unit & formation	Marine/fluvial ratio	Channel geometry	Channel %	Channel width (m)	Channel thickness (m)	Channel W/T ratio	Crevasse splay %	Crevasse splay width (m)	Crevasse splay thickness (m)	Crevasse splay W/T ratio	Overbank %
		0 — 1		0 — 100	0 — 350	0 — 8	0 — 36	0 — 100	0 — 1080	0 — 7	0 — 158	0 — 100
Sequence B	PS:6 Scalby Formation	0.00		39	187	6	26	8	111	0.87	125	53
	PS:5 Scarborough Formation	1.00	—	—	—	—	—	—	—	—	—	—
	PS:4 Scarborough Formation	1.00	—	—	—	—	—	—	—	—	—	—
Sequence A	PS:3 Lebberston & Gristhorpe members	0.50		5	34	4	10.5	53	1080	6.7	158	42
	PS:2 Eller Beck Formation & Sycarham Member	0.20		48	328	8	36	11	151	1.21	127	41
	PS:1 Dogger & Saltwick formations	0.13		50	350	7.5	35	14	185	1.32	143	36

Member (PS 2), typically represent a low A/S where the rate of accommodation creation is low and/or sediment supply is high. Conversely, systems with small, single-storey channels and a high proportion of preserved floodplain fines such as the Gristhorpe (PS 3) and Long Nab (PS 6) members are more typical of systems with very high A/S where rapid subsidence preserves more of the section from reworking by channels. Mjøs and Prestholm (1993) suggested that low accommodation as a result of low subsidence or sea-level fall associated with high sediment supply favours vertically incised channel and channel avulsion in a stable channel belt forming these stacked multi-storey channel bodies, whereas the high A/S lead to shallower channel incision and less stable channel formation which creates isolated, low width-to-thickness of the channel body. Alexander (1989) suggested that in a low-lying delta plain like the Cleveland Basin, fluctuation of relative sea level plays an important role in a fluvial stacking pattern. The vertical and lateral stacking of the channel bodies and the relationship to the flooding surfaces and syn-sedimentary faults within Sequence A are considered further below.

Previous authors (Eschard *et al.* 1992a) have suggested that the Moor Grit Member at the base of the Scalby Formation represents an 'incised valley fill'. This interpretation suggests that the A/S is negative for a period of time and, following a relative base-level fall, a valley was cut and sediment was bypassed further downdip. In such a model, the multi-storey fluvial deposits of the Moor Grit Member are laid down as base-level starts to rise, creating accommodation. A further increase in the rate of accommodation results in a transition to more heterolithic channel-fill deposits which may be tidally influenced at the base of the Long Nab Member. Further increase in the A/S resulted in the deposition of the overlying, low-net:gross upper part of the Long Nab Member. The depositional model of Sequence B is similar to the model proposed by Shanley and McCabe (1993) where the base-level change

controls the fluvial architecture. For the interpretation of the incised valley to be confirmed, it would be necessary to map out valley margins and interfluves and to map a lowstand shoreline further basinward. While this is not possible with the data available, the valley model is supported by (i) the presence of a biostratigraphically confirmed unconformity at the base (Leeder and Nami 1979) and (ii) a demonstrable change in accretion bar style from clean sandstone-dominated thick channel bars at the base (basal part of Moor Grit Member) to the downstream-translated point bars at the middle to the heterolithic deposits of the less confined expanding point bar at the upper part (Eschard *et al.* 1992a; Ielpi and Ghinassi 2014).

Syn-tectonic sedimentation in the Ravenscar Group

Previous studies have interpreted the degree of channel amalgamation (i.e. reoccupation of channels of the same location through time) and lateral facies variation in the Ravenscar Group to be controlled by syn-depositional movement on the Whitby and Peak faults (Fig. 20a; Alexander 1986; Alexander and Gawthorpe 1993). In these interpretations, the multi-storey channel bodies were thought to have been formed as a result of preferential stacking of channels in the hangingwall, associated with a marked change in formation thickness across the faults.

In the Whitby East Cliff, the Saltwick Formation is 28 m thick. In the Whitby West Cliff section, neither the Dogger nor the Eller Beck formations are exposed, but there is a 20 m thick multi-storey amalgamated Saltwick Formation channel body present. This rapid facies change was used by Rawson and Wright (1992) to invoke a NNW–SSE-trending fault along the River Esk, and Alexander and Gawthorpe (1993) proposed that the fault was responsible for the changes in facies stacking patterns. There has been discussion concerning the throw of the fault, if present. Hemingway *et al.*
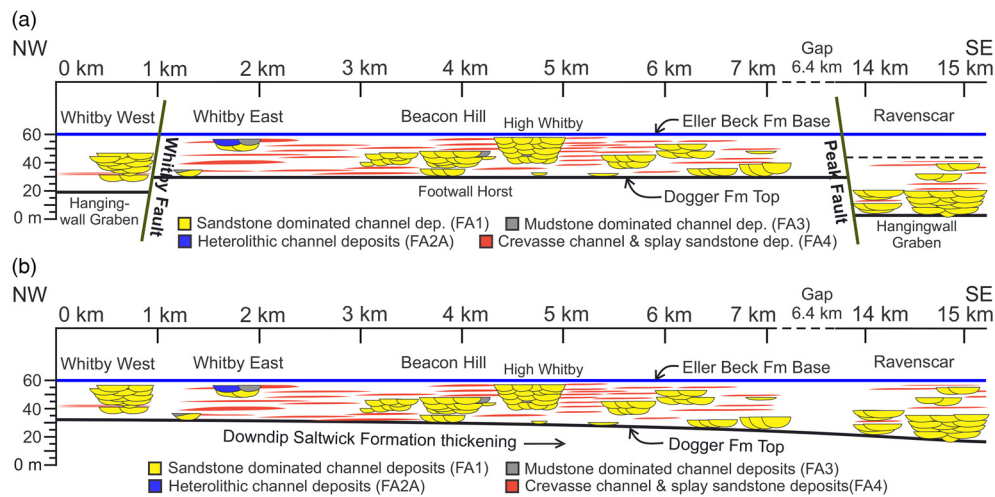
Fig. 20. Controls of fault on channel architecture and variation of formation thickness. (**a**) Scenario-1: distribution of channel bodies with syndepositional fault movement where the Whitby Fault displacement is described as 12 m and the Peak Fault as 27 m and Saltwick Formation thickness increases in the hangingwall block as 12 and 27 m respectively in Whitby West Cliff and Ravenscar East Cliff (Alexander and Gawthorpe 1993). Between these two faults is the horst, but several thick multi-storey channel bodies (up to 20 m thick) are observed in the horst, which is unusual. (**b**) Scenario-2: simple downdip thickening. The channel bodies shifted through time due to normal accommodation-controlled channel avulsion. The formation thickness increased from 28 m at Whitby East Cliff through 33 m at Beacon Hill Cliff to 43 m at Ravenscar East Cliff due to downdip stratigraphic thickening of the Saltwick Formation.

(1968) and Rawson and Wright (1992) suggested that the Dogger Formation is not more than 12 m below the present foreshore on the west side and in a more recent study Kulpecz (2008) described no significant formation thickening across the fault along the course of the River Esk. In this study, we did not observe any evidence of significant thickening of the Saltwick Formation across the Whitby Faults on the virtual outcrops. Furthermore, the occurrence of large, stacked and amalgamated channel bodies, which have previously been described as evidence for fault movement, also occur in several other sections such as Beacon Hill, where the virtual outcrop shows no evidence for fault movement. Therefore, we suggest that there is no evidence that the Whitby Fault controlled or influenced sedimentation.

Further south, previous studies reported that the thickness of the Saltwick Formation increased from 30 m to 57 m across the Peak Fault at Ravenscar (Hemingway 1974). The virtual outcrop supports this increase in thickness but suggests that it is less, 13 m from 30 m in the footwall (considering 30 m of formation thickness developed in the west of the fault) to 43 m in the hangingwall.

Detail of the stratal relationships around the Peak Fault are obscured by poor outcrop. Determining thickness variations of the Saltwick Formation across the fault was not possible due to the absence of Eller Beck Formation exposure in the footwall side of the fault. Consequently, two models that explain the thickening of the Saltwick Formation towards the SE are considered.

Syn-depositional fault movement

There is clear evidence that Peak Fault was active during the deposition of the Dogger Formation and there is demonstratable thinning on to the footwall block (Hemingway 1974; Milsom and Rawson 1989). Evidence for continued movement during the deposition of Saltwick is less clear. There is an apparent thickening, although this is less than previously described and there is a change in channel-stacking patterns with a series of large, multi-storey channel bodies being deposited in the hangingwall block of the fault (Fig. 20a). These channel bodies have previously been cited as evidence that fluvial systems were trapped against the fault scarp (Alexander 1986; Alexander and Gawthorpe 1993) and unable to avulse laterally. However, as with the Whitby Fault, comparable stacked channel bodies are seen in numerous places along the coast where they are demonstrably not associated with faults or fault scarps.

Simple downdip thickening

At Whitby East cliff, the Saltwick Formation is 28 m thick; at the Beacon Hill section, about 4 km SE of the Whitby Fault the formation is up to c. 33 m thick and further 8 km SE at Ravenscar the thickness has increased to 43 m. These values illustrate a general, downdip thickening of 1.25 m km^{-1} (Fig. 20b). The complete sections 22 km long on either side of the Peak Fault suggest that the observed 13 m of thickening could simply be part of this trend.

Faults as a secondary control on channel belt location

As stated above, it is clear that the Peak Fault was active during deposition of the Dogger Formation but less certain during Saltwick times. It is possible that locally, either through differential compaction of the underlying, thicker, Dogger Formation, or minor faulting, that the Peak Fault influenced the location of the major stacked channel bodies in its hangingwall. However, deposition is also influenced by the regional floodplain tilting and base level changes.

A similar scenario has also been seen in the age-equivalent Ness Formation in the Norwegian North Sea (Johnsen *et al.* 1995; Ryseth 2000). Both the preferential occurrence of channel bodies, in hangingwall blocks, parallel to minor faults, and the main channel bodies that either cut directly over faults and ignore them or are developed away from faults, were studied there.

Both cases (Saltwick Formation in Yorkshire and Ness Formation in the North Sea) suggest that faults had limited surface expression during deposition. The depositional systems will infill any subtle topographic lows associated with the faults and may locally impact channel location, but overall the coastal plain drainage systems were capable of ignoring the faults and were able to be more controlled by, e.g., the base level changes or overall tilt of the coastal plain from the land towards the sea (Ryseth 2000; Mack *et al.* 2003).

The fluvio-deltaic Sycarham and Gristhorpe members of the Cloughton Formation and the Scalby Formation sections do not have an extensive enough dataset to explore the influence of the syndepositional fault movement and preferential channel development.

The channel body morphology-changing pattern from broad, thick, multi-storeyed channel body to isolated, small channels stacked in floodplain fines or vice versa in vertical section and decreasing channel body dimension towards depositional dip indicate that base level changes or overall tilt of the coastal plain from the land towards the sea may play an important role, for example, in the Saltwick Formation.

Architecture of overbank sandbodies and their role in paralic reservoirs

Crevasse splays are the primary coarse-grained architectural element in overbank deposits. Three different splay geometries: single splays, amalgamated splays and splay complexes are categorized based on their stacking pattern. Single splays are small-scale, isolated, lenticular or sheet-like sandbodies. The *length/width* ratio of single-splay bodies suggests a lobate geometry. Crevasse splays studied in modern systems (Rahman 2019, ch.2), also show lobate single-splay geometries in similar climatic settings (humid to subtropical) to these in fluvio-deltaic deposits. Amalgamation of splays form moderate to large sandbodies which show three different splay stacking patterns. Vertically amalgamated splays are up to 3.8 m thick sandstone sheets where the individual splays are separated by erosional contact or rooted horizons which suggest an amalgamation of two separate splays. In laterally amalgamated splays, individual splays are connected to the contiguous splays and form lensoid, boudinage geometry in cross-section. Both the lateral and vertical

amalgamation processes form comparatively thicker (up to 5.8 m), stacked sandbodies where the individual splays are connected laterally and vertically with pockets of floodplain mudstones. Amalgamated splays developed as a result of compensational stacking in the high accommodation parent channel systems (van Toorenenburg *et al.* 2016; Gulliford *et al.* 2017).

The observed crevasse splay complexes are the thickest (up to 6.5 m) and most extensive (>1200 m wide at the Cloughton Wyke section; Mjøs *et al.* 1993 reported *c.* 20 km) overbank sandbodies. The coarsening upward trend and tidal indicator sedimentary structures (flaser, lenticular and wavy beddings) suggest the splay progradation in the interdistributary bay is similar to that of the crevasse splay complexes in the modern Mississippi Delta (Rahman 2019, ch.2).

Splays constitute a significant proportion of all of the studied delta plain successions (up to 28% in the Saltwick Formation at Whitby East Cliff and 53% in the Gristhorpe Member at Cloughton Wyke). The volume of crevasse splay deposits was estimated from the studied dimensional data. The single-crevasse splays have a larger aerial extent but comperatively low volumes (10^2–10^5 m^3) because they are thin. The amalgamated crevasse splays which formed as a result of lateral and vertical stacking of single splays attain several metres thick sandbody with parent channel parallel large aerial extent, and their rock volumes range on the order of 10^2–10^6 m^3. Donselaar *et al.* (2013), Li *et al.* (2014) and van Toorenenburg *et al.* (2016) also reported splay volumes on the order of 10^6 m^3. The crevasse splay complexes are aerially
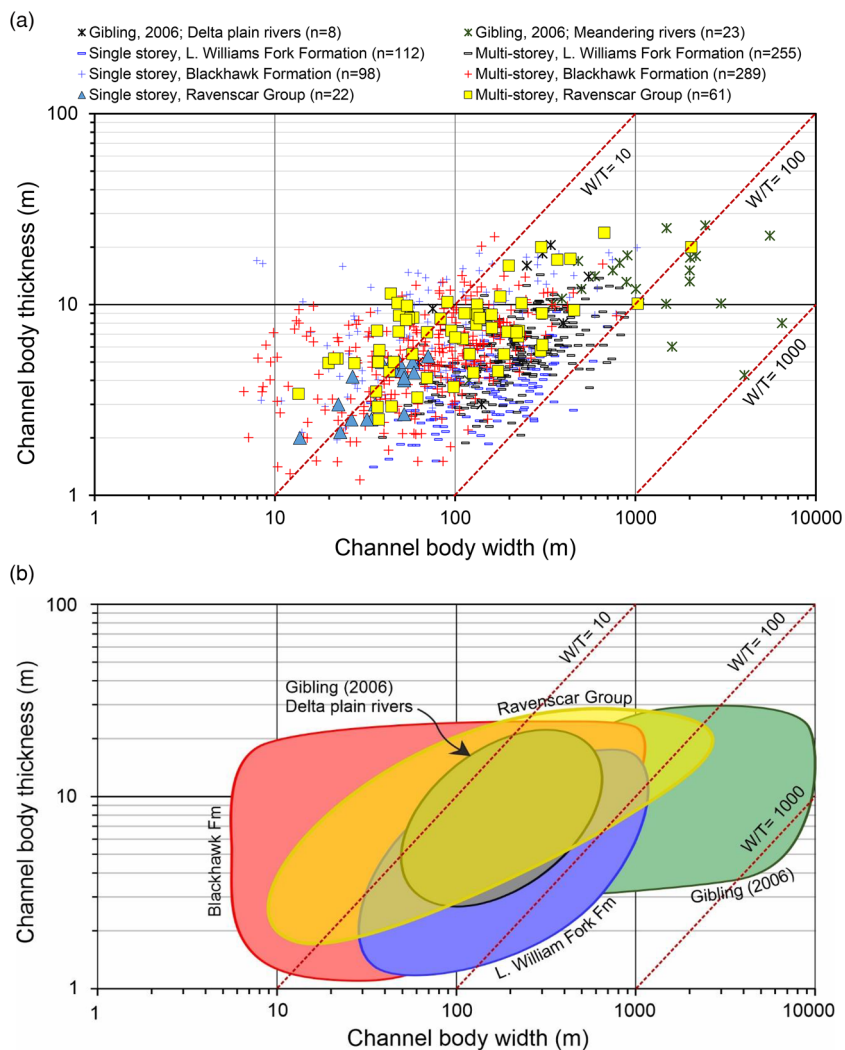

Fig. 21. Comparison of *W/T* values of channel bodies. (**a**) *W/T* plot of channel bodies in the fluvio-deltaic successions of the Ravenscar Group and previously studied sections from similar depositional environments; (**b**) comparison of *W/T* values.
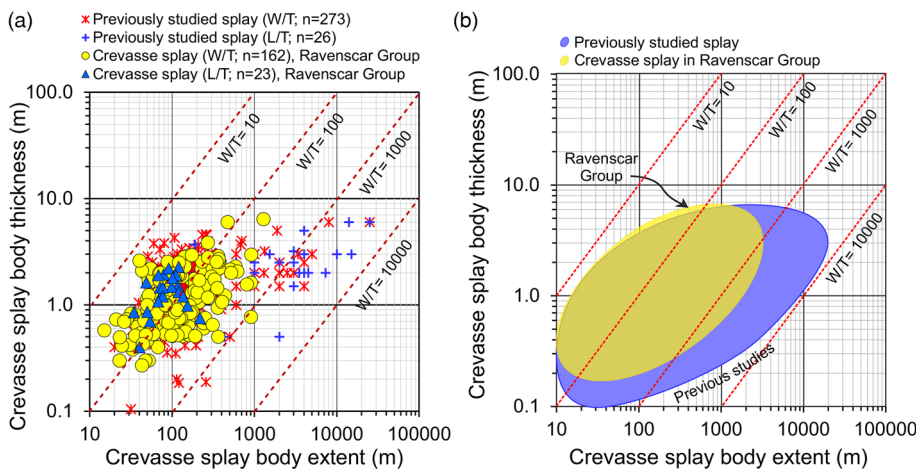
Fig. 22. Comparison of *W/T* values of crevasse splay bodies. (**a**) Cross-plot of *W/T* of crevasse splay and crevasse channel bodies in the Ravenscar Group and previously studied splay bodies; (**b**) comparison of *W/T* values.

extensive bodies with a thickness up to 6.5 m, and with their rock volume on the order of >10^7 m^3. Mjøs *et al.* (1993) suggested their rock volume to be up to 10^9 m^3 in the Gristhorpe Member. Coeval splay bodies are connected to the parent channel and occasionally truncated by the younger channel, providing channel body connectivity. In the delta plain/paralic settings splays may enhance the reservoir volume and occasionally reservoir connectivity.

Comparison of sandbody dimension with analogues

The dimensional data of studied sandbodies were analysed within a broader context by comparing with channel body dimensions of similar depositional environments from published literature. Channel body dimensions were compared with data from delta plain and meandering river systems, compiled by Gibling (2006), lower coastal plain deposits of the Lower Williams Fork Formation, studied by Pranter *et al.* (2009) and fluvial and coastal plain successions of the Blackhawk Formation, studied by Rittersbacher *et al.* (2014) (Fig. 21).

The channel body dimensions of the fluvio-deltaic succession of the Ravenscar Group show similarity with previously studied systems in similar depositional environments (Fig. 21). The compiled delta plain channel body *W/T* of Gibling (2006) are entirely placed within the *W/T* envelope of the Ravenscar Group. Gibling (2006) reported that delta plain distributaries are 3–20 m thick with *W/T* <50 which are characterized by predominant vertical accretion. However, the delta plain channel body dimensions in the Ravenscar Group are widely distributed, ranging from 15–2034 m wide and 3–28 m thick with *W/T* 5–>102. They are characterized by predominant lateral accretion. The dominance of multi-storey channel body types along with point bar deposits imply that most of the channel bodies are laterally migrated and vertically or obliquely stacked.

As the studied channel bodies in the Ravenscar Group are dominated by lateral accretion deposits they were compared to the meandering channel body dimensions of Gibling (2006). The *W/T* values of some of the largest channel bodies in the Ravenscar Group (for example, channel bodies in the lower part of the Saltwick Formation and exhumed meander belt of the Scalby Formation) are comparable to the lower-end members of meandering channel bodies. The valley-fill deposits of the Moor Grit Member (>1000 m wide, 10 m thick with *W/T* >100) are similar to the 'Valley Fill within Alluvial and Marine Strata' type of Gibling (2006).

The channel bodies of the coastal plain Lower Williams Fork Formation, Coal Canyon, Colorado (Pranter *et al.* 2009), mostly show a similar distribution to the Ravenscar Group. The single-storey channel bodies in the Lower Williams Fork Formation are

1.2–9.1 m thick and 14–518 m wide with *W/T* 6–150, whereas the single-storey channel bodies in the Ravenscar Group always show *W/T* <15. The multi-storey channel bodies in the Lower Williams Fork Formation are 16.5–851 m wide and 1.5–14.5 m thick with *W/T* 4–221, whereas those in the Ravenscar Group have *W/T* 15–>102.

Data from the Ravenscar Group show a similar trend to the Blackhawk Formation in the Wasatch Plateau, USA (Rittersbacher *et al.* 2014). In the Blackhawk Formation, Rittersbacher *et al.* (2014) showed that channel bodies are 7–1020 m wide and 2–23 m thick with *W/T* up to 90, which cover most of the envelope of the Ravenscar Group. The channel bodies in the Blackhawk Formation show an increasing upward trend similar to that in the Sycarham Member of the Coughton Formation whereas the Saltwick and Scalby formations show a decreasing upward trend.

Crevasse splay body dimensions of different fluvio-deltaic successions in the Ravenscar Group show a similar trend to those in previous studies (Fig. 22). Previously studied dimensional data of crevasse splays suggest they may extend up to 25 km with thickness up to 6 m and *W/T* up to 4170 (Kerr 1990; Mjøs *et al.* 1993; Smith 1993; Jorgensen and Fielding 1996; Anderson 2005; Arco *et al.* 2006; Pranter *et al.* 2014; Burns *et al.* 2017; Gulliford *et al.* 2017). In the present study, observed crevasse splay bodies are up to >1285 m wide and 6.5 m thick with *W/T* ratio >541. The similarity of the sandbody dimensions of the Ravenscar Group with those of the equivalent depositional environments demonstrates that the studied fluvio-deltaic sections can act as an appropriate analogue for the North Sea reservoirs or any reservoirs deposited in similar environments.

Conclusions

The application of digital data acquisition techniques along with traditional field techniques and behind outcrop well data is a powerful approach to study large and inaccessible cliff exposures even in areas that have been previously well studied. Virtual outcrops provide a means to observe the large-scale geobody trends that are not otherwise obvious, and provide access to otherwise inaccessible sections such as the Jurassic successions of the Yorkshire coast. The studied succession is subdivided into two, unconformity-bounded sequences, and the lower sequence is comprised of five upward-shallowing successions, bounded by marine flooding surfaces. Both sequences show an overall retrogradational stacking pattern. Overall, the entire stratigraphic section shows a thickening down depositional-dip.

The fluvial sandbodies within the succession have been classified into five architectural types: single-storey small ribbon, single-storey broad ribbon, tabular multilateral sheet, internally amalgamated multi-storey sheet and partially amalgamated multi-storey

sheet. These show a systematic arrangement within the para-sequences. Overbank sandbodies have also been mapped. These include ribbon crevasse channels, single-splay sheets, amalgamated splay sheets, crevasse splay sheet complexes and wedge-shaped levee deposits. Dimensional data collected from the sandbodies have utility as an analogue for similar fluvial reservoirs such as the Ness Formation in the Brent Group (North Sea) and the Middle Jurassic Åre Formation in the Norwegian Sea.

Finally, the more complete dataset available from the virtual outcrop studies suggests that previous models for structural controls on channel body distribution may not be correct, especially in the case of the Whitby Fault. While major sandbodies do occur adjacent to the fault, they are not unique to this position, and similar bodies occur in other sections where no faults are observed. There is clear evidence for pre-Saltwick movement on the Peak Fault and potential that faulting continued through Saltwick times; however, faulting is considered to be a local, rather than regional, control on sedimentation patterns.

Scientific editing by Yvonne Spychala

References

Alexander, J. 1986. Idealised flow models to predict alluvial sandstone body distribution in the Middle Jurassic Yorkshire Basin. *Marine and Petroleum Geology*, **3**, 298–305, https://doi.org/10.1016/0264-8172(86)90034-6

Alexander, J. 1989. Delta or coastal plain? With an example of the controversy from the Middle Jurassic of Yorkshire. *Geological Society, London, Special Publications*, **41**, 11–19, https://doi.org/10.1144/GSL.SP.1989.041.01.02

Alexander, J. 1992*a*. A discussion of alluvial sandstone body characteristics related to variations in marine influence, Middle Jurassic of the Cleveland Basin, UK, and the implications for analogous Brent Group strata in the North Sea Basin. *Geological Society, London, Special Publications*, **61**, 149–167, https://doi.org/10.1144/GSL.SP.1992.061.01.09

Alexander, J. 1992*b*. Nature and origin of a laterally extensive alluvial sandstone body in the Middle Jurassic Scalby Formation. *Journal of the Geological Society, London*, **149**, 431–441, https://doi.org/10.1144/gsjgs.149.3.0431

Alexander, J. and Gawthorpe, R.L. 1993. The complex nature of a Jurassic multistorey, alluvial sandstone body, Whitby, North Yorkshire. *Geological Society, London, Special Publications*, **73**, 123–142, https://doi.org/10.1144/GSL.SP.1993.073.01.08

Allen, J.R.L. 1963. The classification of cross-stratified units with notes on their origin. *Sedimentology*, **2**, 93–114, https://doi.org/10.1111/j.1365-3091.1963.tb01204.x

Allen, J.R.L. 1978. Studies in fluviatile sedimentation: an exploratory quantitative model for the architecture of avulsion-controlled alluvial suites. *Sedimentary Geology*, **21**, 129–147, https://doi.org/10.1016/0037-0738(78)90002-7

Allen, J.R.L. 1983. Studies in fluviatile sedimentation: bars, bar-complexes and sandstone sheets (low-sinuosity braided streams) in the brownstones (L.

devonian), welsh borders. *Sedimentary Geology*, **33**, 237–293, https://doi.org/10.1016/0037-0738(83)90076-3

Ambrose, W.A., Lakshminarasimhan, S., Holtz, M.H., Núñez-López, V., Hovorka, S.D. and Duncan, I. 2008. Geologic factors controlling CO₂ storage capacity and permanence: case studies based on experience with heterogeneity in oil and gas reservoirs applied to CO₂ storage. *Environmental Geology*, **54**, 1619–1633, https://doi.org/10.1007/s00254-007-0940-2

Anderson, D.S. 2005. Architecture of crevasse splay and point-bar bodies of the nonmarine Iles Formation north of Rangely, Colorado: implications for reservoir description. *The Mountain Geologist*, **42**, 109–122.

Arco, L.J., Adelsberger, K.A., Hung, L. and Kidder, T.R. 2006. Alluvial geoarchaeology of a middle archaic mound complex in the Lower Mississippi Valley, U.S.A. *Anthropocene*, **4**, 151–153, https://doi.org/10.1002/GEA

Black, M. 1934. Sedimentation of the Aalenian rocks of Yorkshire. *Proceedings of the Yorkshire Geological Society*, **22**, 265–279, https://doi.org/10.1144/pygs.22.4.265

Blakey, R.C. and Gubitosa, R. 1984. Controls of sandstone body geometry and architecture in the Chinle Formation (Upper Triassic), Colorado Plateau. *Sedimentary Geology*, **38**, 51–86, https://doi.org/10.1016/0037-0738(84)90074-5

Bown, T.M. and Kraus, M.J. 1987. Integration of channel and floodplain suites, I. Developmental sequence and lateral relations of alluvial paleosols. *Journal of Sedimentary Petrology*, **57**, 587–601.

Bray, R.J., Green, P.F. and Duddy, I.R. 1992. Thermal history reconstruction using apatite fission track analysis and vitrinite reflectance: a case study from the UK East Midlands and Southern North Sea. *Geological Society, London, Special Publications*, **67**, 3–25, https://doi.org/10.1144/GSL.SP.1992.067.01.01

Bridge, J.S. 1984. Large-scale facies sequences in alluvial overbank environments. *Journal of Sedimentary Research*, **54**, 583–588, https://doi.org/10.1306/212F8477-2B24-11D7-8648000102C1865D

Bridge, J.S. 2006. Fluvial facies models: recent developments. *In*: Posamentier, H. and Walker, R.G. (eds) *Facies models revisited*. SEPM Special Publication, **84**, 85–170, https://doi.org/10.2110/pec.06.84.0019

Bridge, J.S. and Tye, R.S. 2000. Interpreting the dimensions of ancient fluvial channel bars, channels, and channel belts from wireline-logs and cores. *AAPG Bulletin*, **84**, 1205–1228, https://doi.org/10.1306/a9673c84-1738-11d7-8645000102c1865d

Bristow, C.S., Skelly, R.L. and Ethridge, F.G. 1999. Crevasse splays from the rapidly aggrading, sand-bed, braided Niobrara River, Nebraska: effect of base-level rise. *Sedimentology*, **46**, 1029–1047, https://doi.org/10.1046/j.1365-3091.1999.00263.x

Buckley, S.J., Howell, J.A., Enge, H.D. and Kurz, T.H. 2008. Terrestrial laser scanning in geology: data acquisition, processing and accuracy considerations. *Journal of the Geological Society*, **165**, 625–638, https://doi.org/10.1144/0016-76492007-100

Buckley, S.J., Schwarz, E., Terlaky, V., Howell, J.A. and Arnott, R.W. 2010. Combining Aerial photogrammetry and Terrestrial lidar for reservoir analog modeling. *Photogrammetric Engineering and Remote Sensing*, **76**, 953–963, https://doi.org/10.14358/PERS.76.8.953

Buckley, S.J., Ringdal, K., Naumann, N., Dolva, B., Kurz, T.H., Howell, J.A. and Dewez, T.J.B. 2019. LIME: software for 3-D visualization, interpretation, and communication of virtual geoscience models. *Geosphere*, **15**, 1–14, https://doi.org/10.1130/GES02002.1/4610849/ges02002.pdf

Burns, C.E., Mountney, N.P., Hodgson, D.M. and Colombera, L. 2017. Anatomy and dimensions of fluvial crevasse-splay deposits: examples from the Cretaceous Castlegate Sandstone and Neslen Formation, Utah, U.S.A. *Sedimentary Geology*, **351**, 21–35, https://doi.org/10.1016/j.sedgeo.2017.02.003

Burns, C.E., Mountney, N.P., Hodgson, D.M. and Colombera, L. 2019. Stratigraphic architecture and hierarchy of fluvial overbank splay deposits. *Journal of the Geological Society Stratigraphic*, **176**, 629–649, https://doi.org/10.1144/jgs2019-001

Butler, N., Charnock, M.A., Hager, K.O. and Watkins, C.A. 2005. The Ravenscar Group : a coeval analogue for the Middle Jurassic reservoirs of the North Sea and offshore Mid-Norway. *In*: Powell, A.J. and Riding, J.B. (eds) *Recent Developments in Applied Biostratigraphy*. *The Micropalaeontological Society, Special Publications*, 43–53.

Campbell, C. V. 1976. Reservoir geometry of a fluvial sheet sandstone. *AAPG Bulletin (American Association of Petroleum Geologists)*, **60**, 1009–1020, https://doi.org/10.1306/c1ea3609-16c9-11d7-8645000102c1865d

Choi, K., Jackson, M.D., Hampson, G., Jones, A.D.W. and Reynolds, T. 2007. Impact of heterogeneity on flow in fluvial-deltaic reservoirs – implications for the giant ACG field, South Caspian Basin. Paper SPE 107137, presented at the 69th European Association of Geoscientists and Engineers Conference and Exhibition, 11–14 June, London, UK, https://doi.org/10.2118/107137-ms

Cope, J.C.W., Duff, K.L., Parsons, C.F., Torrens, H.S., Wimbledon, W.A. and Wright, J.K.A. 1980. A correlation of Jurassic rocks in the British Isles, Part 2: middle and Upper Jurassic. *Geological Society of London, Special Publications*, **15**, 109.

Cox, B.M. and Sumbler, M.G. 2002. *British Middle Jurassic Stratigraphy*. Joint Nature Conservation Committee: Geological Conservation Review Series, 26.

Demko, T.M., Currie, B.S. and Nicoll, K.A. 2004. Regional paleoclimatic and stratigraphic implications of paleosols and fluvial/overbank architecture in the

Morrison Formation (Upper Jurassic), Western Interior, USA. *Sedimentary Geology*, **167**, 115–135, https://doi.org/10.1016/j.sedgeo.2004.01.003

Donselaar, M.E., Cuevas Gozalo, M.C. and Moyano, S. 2013. Avulsion processes at the terminus of low-gradient semi-arid fluvial systems: lessons from the Río Colorado, Altiplano endorheic basin, Bolivia. *Sedimentary Geology*, **283**, 1–14, https://doi.org/10.1016/j.sedgeo.2012.10.007

Doyle, J.D. and Sweet, M.L. 1995. Three-dimensional distribution of lithofacies, bounding surfaces, porosity, and permeability in a fluvial sandstone – Gypsy Sandstone of northern Oklahoma. *American Association of Petroleum Geologists Bulletin*, **79**, 70–96, https://doi.org/10.1306/8D2B14BC-171E-11D7-8645000102C1865D

Dreyer, T., Scheie, A. and Walderhaug, O. 1990. Minipermeameter-based study of permeability trends in channel sand bodies. *American Association of Petroleum Geologists Bulletin*, **74**, 359–374, https://doi.org/10.1306/0C9B22F9-1710-11D7-8645000102C1865D

Eaton, T.T. 2006. On the importance of geological heterogeneity for flow simulation. *Sedimentary Geology*, **184**, 187–201, https://doi.org/10.1016/j.sedgeo.2005.11.002

Elliott, T. 1974. Interdistributary bay sequences and their genesis. *Sedimentology*, **21**, 611–622, https://doi.org/10.1111/j.1365-3091.1974.tb01793.x

Enge, H.D., Buckley, S.J., Rotevatn, A. and Howell, J.A. 2007. From outcrop to reservoir simulation model: workflow and procedures. *Geosphere*, **3**, 469–490, https://doi.org/10.1130/GES00099.1

Enge, H.D., Howell, J.A. and Buckley, S.J. 2010. The Geometry and Internal Architecture of Stream Mouth Bars in the Panther Tongue and the Ferron Sandstone Members, Utah, U.S.A. *Journal of Sedimentary Research*, **80**, 1018–1031, https://doi.org/10.2110/jsr.2010.088

Eschard, R., Ravenne, C., Houel, P. and Knox, R. 1992*a*. Three-dimensional reservoir architecture of a valley-fill sequence and a deltaic aggradational sequence: influences of minor relative sea-level variations (Scalby Formation, England). *In*: Miall, A.D. and Tyler, N. (eds) *The Three-Dimensional Facies Architecture of Terrigenous Clastic Sediments and Its Implications for Hydrocarbon Discovery and Recovery*. SEPM, **3**, 133–147, https://doi.org/10.2110/csp.91.03.0122

Eschard, R. and Heresim Group 1992*b*. High resolution sequence stratigraphy and reservoir characterisation of a deltaic system from outcrops, Cores and Logs, Cleveland Basin, UK. *In*: Eschard, R. and Doligez, B. (eds) *Subsurface Reservoir Characterisation from Outcrop Observations*. 7th IFP Exploration Production Research Conference Proceedings, April 1992, Paris, 71.

Fabuel-Perez, I., Hodgetts, D. and Redfern, J. 2009. A new approach for outcrop characterization and geostatistical analysis of a low-sinuosity fluvial-dominated succession using digital outcrop models: Upper triassic oukaime-den sandstone formation, central high Atlas, Morocco. *AAPG Bulletin*, **93**, 795–827, https://doi.org/10.1306/02230908102

Farrell, K.M. 1987. Sedimentology and facies architecture of overbank deposits of the Mississippi River, False River Region, Louisiana. *In*: Ethridge, F.G., Flores, R.M. and Harvey, M.D. (eds) *Recent Developments in Fluvial Sedimentology*. The Society of Economic Paleontologists and Mineralogists, **39**, 111–120.

Fielding, C.R. 1984. Upper delta plain lacustrine and fluviolacustrine facies from the Westphalian of the Durham coalfield, NE England. *Sedimentology*, **31**, 547–567, https://doi.org/10.1111/j.1365-3091.1984.tb01819.x

Fielding, C.R. 1986. Fluvial channel and overbank deposits from the Westphalian of the Durham coalfield, NE England. *Sedimentology*, **33**, 119–140, https://doi.org/10.1111/j.1365-3091.1986.tb00748.x

Fisher, M.J. and Hancock, N.J. 1985. The Scalby Foormation (Middle Jurassic, Ravenscar Group) of Yorkshire: reaassessment of age and depositional environment. *Proceedings of the Yorkshire Geological Society*, **45**, 293–298, https://doi.org/10.1144/pygs.45.4.293

Ford, G.L. and Pyles, D.R. 2014. A hierarchical approach for evaluating fluvial systems: Architectural analysis and sequential evolution of the high net-sand content, middle Wasatch Formation, Uinta Basin, Utah. *AAPG Bulletin*, **98**, 1273–1304, https://doi.org/10.1306/12171313052

Friend, F., Slater, M.J. and Williams, R.C. 1979. Vertical and lateral building of river sandstone bodies, Ebro Basin, Spain. *Journal of the Geological Society*, **136**, 39–46, https://doi.org/10.1144/gsjgs.136.1.0039

Gibling, M.R. 2006. Width and thickness of fluvial channel bodies and valley fills in the geological record: a literature compilation and classification. *Journal of Sedimentary Research*, **76**, 731–770, https://doi.org/10.2110/jsr.2006.060

Gouw, M.J.P. and Autin, J.W. 2008. Alluvial architecture of the Holocene Rhine-Meuse delta (the Netherlands). *Sedimentology*, **55**, 1487–1516, https://doi.org/10.1111/j.1365-3091.2008.00954.x

Gouw, M.J.P. and Berendsen, H.J.A. 2007. Variability of channel-belt dimensions and the consequences for alluvial architecture: Observations from the Holocene Rhine-Meuse Delta (The Netherlands) and Lower Mississippi Valley (U.S.A.). *Journal of Sedimentary Research*, **77**, 124–138, https://doi.org/10.2110/jsr.2007.013

Gowland, S. and Riding, J.B. 1991. Stratigraphy, sedimentology and palaeontology of the Scarborough Formation (Middle Jurassic) at Hundle point, North Yorkshire. *Proceedings of the Yorkshire Geological Society*, **48** , 375–392, https://doi.org/10.1144/pygs.48.4.375

Green, P.F. 1986. On the thermotectonic evolution of northern England: evidence from fission-track analysis. *Geological Magazine*, **123**, 493–506, https://doi.org/10.1017/S0016756800035081

Gulliford, A.R., Flint, S.S. and Hodgson, D.M. 2017. Crevasse splay processes and deposits in an ancient distributive fluvial system: the lower Beaufort Group, South Africa. *Sedimentary Geology*, **358**, 1–18, https://doi.org/10.1016/j.sedgeo.2017.06.005

Hajek, E.A. and Edmonds, D.A. 2014. Is river avulsion style controlled by floodplain morphodynamics? *Geology*, **42**, 199–202, https://doi.org/10.1130/G35045.1

Hancock, N. and Fisher, M. 1981. Middle Jurassic North Sea Deltas with Particular Reference to Yorkshire. *In*: Illing, L.V. and Hobson, G.D. (eds) *Petroleum Geology of the Continental Shelf of North-West Europe*. Institute of Petroleum, London, 186–193.

Hartley, A.J., Weissmann, G.S., Nichols, G.J. and Warwick, G.L. 2010. Large distributive fluvial systems: characteristics, distribution, and controls on development. *Journal of Sedimentary Research*, **80**, 167–183, https://doi.org/10.2110/jsr.2010.016

Hemingway, J.E. 1974. Jurassic. *In*: Raynor, D.H. and Hemingway, J.E. (eds) *The Geology and Mineral Resources of Yorkshire*. Yorkshire Geological Society, Leeds, 161–233.

Hemingway, J.E. and Knox, R.W.O. 1973. Lithostratigraphical nomenclature of the Middle Jurassic strata of the Yorkshire Basin of North-East England. *Proceedings of the Yorkshire Geological Society*, **39**, 527–535, https://doi.org/10.1144/pygs.39.4.527

Hemingway, J.E. and Riddler, G.P. 1982. Basin inversion in North Yorkshire. *Transactions of the Institute of Mining and Metallurgy*, **91**, 175–186.

Hemingway, J.E., Wilson, V. and Wright, C.W. 1968. *Geology of the Yorkshire Coast*. Geologists' Association Guides, Benham, Colchester, 34.

Hesselbo, S.P., Morgans-Bell, H.S., McElwain, J.C., Rees, P.M., Robinson, S.A. and Ross, C.E. 2003. Carbon-cycle perturbation in the Middle Jurassic and Accompanying Changes in the Terrestrial Paleoenvironment. *The Journal of Geology*, **111**, 259–276, https://doi.org/10.1086/373968

Hirst, J.P.P. 1991. Variations in Alluvial Architecture Across the Oligo-Miocene Huesca Fluvial System, Ebro Basin, Spain. *In*: Miall, A.D. and Tylers, C.N. (eds) *The Three Dimensional Facies Architecture of Heterogeneous Clastic Sediments and its Implications for Hydrocarbon Discovery and Recovery*. Concepts Sedimentol. Palontol., **3**, 111–121, https://doi.org/10.2110/csp.91.03.0103

Hodgetts, D. 2013. Laser scanning and digital outcrop geology in the petroleum industry: a review. *Marine and Petroleum Geology*, **46**, 335–354, https://doi.org/10.1016/j.marpetgeo.2013.02.014

Holbrook, J., Scott, R.W. and Oboh-Ikuenobe, F.E. 2006. Base-level buffers and buttresses: a model for upstream versus downstream control on fluvial geometry and architecture within sequences. *Journal of Sedimentary Research*, **76**, 162–174, https://doi.org/10.2110/jsr.2005.10

Howell, J.A., Chmielewska, M., Lewis, C., Buckley, S.J., Naumann, N. and Pugsley, J. 2021. Acquisition of data for building photogrammetric virtual outcrop models for the geosciences using remotely piloted vehicles (RPVs). *EarthArXiv*, 1–14, https://doi.org/10.31223/X54914

Ielpi, A. and Ghinassi, M. 2014. Planform architecture, stratigraphic signature and morphodynamics of an exhumed Jurassic meander plain (Scalby Formation, Yorkshire, UK). *Sedimentology*, **61**, 1923–1960, https://doi.org/10.1111/sed.12122

Issautier, B.Î., Fillacier, S., Le Gallo, Y., Audigane, P., Chiaberge, C. and Viseur, S. 2013. Modelling of CO_2 injection in fluvial sedimentary heterogeneous reservoirs to assess the impact of geological heterogeneities on CO_2 storage capacity and performance. *Energy Procedia*, **37**, 5181–5190, https://doi.org/10.1016/j.egypro.2013.06.434

Jensen, M.A. and Pedersen, G.K. 2010. Architecture of vertically stacked fluvial deposits, Atane Formation, Cretaceous, Nuussuaq, central West Greenland. *Sedimentology*, **57**, 1280–1314, https://doi.org/10.1111/j.1365-3091.2010.01146.x

Jones, H.L. and Hajek, E.A. 2007. Characterizing avulsion stratigraphy in ancient alluvial deposits. *Sedimentary Geology*, **202**, 124–137, https://doi.org/10.1016/j.sedgeo.2007.02.003

Johnsen, J.R., Rutledal, H. and Nilsen, D.E. 1995. Jurassic reservoirs; field examples from the Oseberg and Troll fields: Horda Platform area. *Norwegian Petroleum Society Special Publications*, **4**, 199–234, https://doi.org/10.1016/S0928-8937(06)80043-3

Jorgensen, P.J. and Fielding, C.R. 1996. Facies architecture of alluvial floodbasin deposits: three-dimensional data from the upper triassic callide coal measures of east-central Queensland, Australia. *Sedimentology*, **43**, 479–495, https://doi.org/10.1046/j.1365-3091.1996.d01-25.x

Kantorowicz, J.D. 1990. Lateral and vertical variations in pedogenesis and other early diagenetic phenomena, Middle Jurassic Ravenscar Group, England. *Proceedings of the Yorkshire Geological Society*, **48**, 61–74, https://doi.org/10.1144/pygs.48.1.61

Kent, P.E. 1955. The market weighton structure. *Proceedings of the Yorkshire Geological Society*, **30**, 197–224, https://doi.org/10.1144/pygs.30.2.197

Kent, P.E. 1980. Subsidence and upliftment in East Yorkshire and Lincolnshire: a double inversion. *Proceedings of the Yorkshire Geological Society*, **42**, 505–524, https://doi.org/10.1144/pygs.42.4.505

Keogh, K.J., Martinius, A.W. and Osland, R. 2007. The development of fluvial stochastic modelling in the Norwegian oil industry: a historical review, subsurface implementation and future directions. *Sedimentary Geology*, **202**, 249–268, https://doi.org/10.1016/j.sedgeo.2007.05.009

Keogh, K.J., Leary, S. *et al.* 2014. Data capture for multiscale modelling of the Lourinha Formation, Lusitanian Basin, Portugal: an outcrop analogue for the Statfjord Group, Norwegian North Sea. *Geological Society, London, Special Publications*, **387**, 27–56, https://doi.org/10.1144/SP387.11

Kerr, D.R. 1990. Reservoir heterogeneity in the middle frio formation: case studies in stratton and agua dulce fields, Nueces County, Texas. *Transaction-Gulf Coast Associations of Geological Societies*, **XL**, 363–372.

Kirby, G.A. and Swallow, P.W. 1987. Tectonism and sedimentation in the Flamborough Head region of north-east England. *Proceedings of the Yorkshire Geological Society*, **46**, 301–309, https://doi.org/10.1144/pygs.46.4.301

Knox, R.W.O'B. 1973. The Eller Beck Formation (Bajocian) of the Ravenscar Group of NE Yorkshire. *Geological Magazine*, **110**, 511–534, https://doi.org/10.1017/S0016756800037912

Kraus, M.J. 1987. Integration of channel and floodplain suites, ii. Vertical relations of alluvial paleosols. *Journal of Sedimentary Petrology*, **57**, 602–612.

Kulpecz, A.A. 2008. *Controls on facies architecture in the Middle Jurassic Ravenscar Group, Yorkshire Coast, UK*. PhD thesis, Imperial College London.

Lazar, O.R., Bohacs, K.M., Macquaker, J.H.S., Schieber, J. and Demko, T.M. 2015. Capturing key attributes of fine-grained sedimentary rocks in outcrops, cores, and thin sections: nomenclature and description guidelines. *Journal of Sedimentary Research*, **85**, 230–246, https://doi.org/10.2110/jsr.2015.11

Leeder, M. and Nami, M. 1979. Sedimentary models for the non-marine scalby formation (Middle Jurassic) and evidence for late bajocian/bathonian uplift of the Yorkshire Basin. *Proceedings of the Yorkshire Geological Society*, **42**, 461–482, https://doi.org/10.1144/pygs.42.3.461

Lepre, C.J. 2017. Crevasse-splay and associated depositional environments of the hominin-bearing lower Okote Member, Koobi Fora Formation (Plio-Pleistocene), Kenya. *The Depositional Record*, **3**, 161–186, https://doi.org/10.1002/dep2.31

Li, Y. and Bhattacharya, J. 2014. Facies architecture of asymmetrical branching distributary channels: cretaceous Ferron Sandstone, Utah, USA. *Sedimentology*, **61**, 1452–1483, https://doi.org/10.1111/sed.12104

Li, J., Donselaar, M.E., Hosseini Aria, S.E., Koenders, R. and Oyen, A.M. 2014. Landsat imagery-based visualization of the geomorphological development at the terminus of a dryland river system. *Quaternary International*, **352**, 100–110, https://doi.org/10.1016/j.quaint.2014.06.041

Li, J., Luthi, S.M., Donselaar, M.E., Weltje, G.J., Prins, M.A. and Bloemsma, M.R. 2015. An ephemeral meandering river system: sediment dispersal processes in the Río Colorado, Southern Altiplano Plateau, *Bolivia. Zeitschrift für Geomorphologie*, **59**, 301–317, https://doi.org/10.1127/zfg/2014/0155

Livera, S.E. 1981. *Sedimentology of Bajocian rocks from the Ravenscar Group of Yorkshire*. PhD thesis, University of Leeds, 151–153.

Livera, S.E. and Leeder, M.R. 1981. The Middle Jurassic Ravenscar Group ('Deltaic Series') of Yorkshire: recent sedimentological studies as demonstrated during a field meeting 2–3 May 1980. *Proceedings of the Geologists' Association*, **92**, 241–250, https://doi.org/10.1016/S0016-7878(81)80051-X

Lott, G.K. and Humphreys, B. 1992. The stratigraphy and petrology of Middle Jurassic (Ravenscar Group) sediments in cored boreholes from the north Yorkshire coast. *Proceedings of the Yorkshire Geological and Polytechnic Society*, **49**, 23–40, https://doi.org/10.1144/pygs.49.1.23

Mack, G.H., Seager, W.R. and Leeder, M.R. 2003. Synclinal-horst basins: examples from the southern Rio Grande rift and southern transition zone of southwestern New Mexico, USA. *Basin Research*, **15**, 365–377, https://doi.org/10.1046/j.1365-2117.2003.00212.x

McGowen, J.H. and Garner, L.E. 1970. Physiographic features and stratification types of coarse-grained pointbars: modern and ancient examples. *Sedimentology*, **14**, 77–111, https://doi.org/10.1111/j.1365-3091.1970.tb00184.x

Miall, A.D. 1988. Reservoir heterogeneities in fluvial sandstones: lesson from outcrop studies. *American Association of Petroleum Geologists Bulletin*, **72**, 682–697, https://doi.org/10.1306/703c8f01-1707-11d7-8645000102c1865d

Miall, A.D. 1996. *The Gology of Fluvial Deposits: Sedimentary Facies, Basin Analysis, and Petroleum Geology*. Springer-Verlag, New York, 582.

Milsom, J. and Rawson, P.F. 1989. The Peak Trough – a major control on the geology of the North Yorkshire coast. *Geological Magazine*, **126**, 699, https://doi.org/10.1017/S0016756800007007

Mjøs, R. and Prestholm, E. 1993. The geometry and organization of fluviodeltaic channel sandstones in the Jurassic Saltwick formation, Yorkshire, England. *Sedimentology*, **40**, 919–935, https://doi.org/10.1111/j.1365-3091.1993.tb01369.x

Mjøs, R., Walderhaug, O. and Prestholm, E. 1993. Crevasse splay sandstone geometries in teh Middle Jurassic Ravesncar Group of Yorkshire, UK. *In*: Marzo, M. and Puigdefabregas, C. (eds) *Alluvial Sedimentation*. International Association of Sedimentologists Special Publication, **17**, 167–185.

Morgans, H.S., Hesselbo, S.P. and Spicer, R.A. 2017. The Seasonal Climate of the Early-Middle Jurassic, Cleveland Basin, England. *Palaios*, **14**, 261–272, https://doi.org/10.2307/3515438

Nami, M. 1976. An exhumed Jurassic meander belt from Yorkshire, England. *Geological Magazine*, **113**, 47–52, https://doi.org/10.1017/S0016756800043004

Nami, M. and Leeder, M.R. 1978. Changing channel morphology and magnitude in the Scalby Formation (m. Jurassic) of Yorkshire, England. *Canadian Society of Petroleum Geologists*, Memoir 5, 605–625.

Nichols, G. 2009. *Sedimentology and Stratigraphy*. Wiley-Blackwell, 138.

Nichols, G.J. and Fisher, J.A. 2007. Processes, facies and architecture of fluvial distributary system deposits. *Sedimentary Geology*, **195**, 75–90, https://doi.org/10.1016/j.sedgeo.2006.07.004

Nichols, E.M., Weissmann, G.S., Wawrzyniec, T.F., Frechette, J.D. and Klise, K.A. 2011. Processing of Outcrop-Based LIDAR imagery to characterize heterogeneity for groundwater models. *In*: Martinsen, O.J., Pulham, A.J., Haughton, P.D.W. and Sullivan, M.D. (eds) *Outcrops Revitalized: Tools, Techniques and Applications*. SEPM, **10**, 239–247, https://doi.org/10.2110/sepmcsp.10.239

O'Brien, P.E. and Wells, A.T. 1986. A small, alluvial crevasse splay. *Journal of Sedimentary Research*, **56**, 876–879, https://doi.org/10.1306/212F8A71-2B24-11D7-8648000102C1865D

Owen, A., Nichols, G.J., Hartley, A.J., Weissmann, G.S. and Scuderi, L.A. 2015. Quantification of a distributive fluvial system: the Salt Wash DFS of the Morrison. *SEPM Journal of Sedimentary Research*, **85**, 544–561, https://doi.org/10.2110/jsr.2015.35

Owen, A., Ebinghaus, A., Hartley, A.J., Santos, M.G.M. and Weissmann, G.S. 2017. Multi-scale classification of fluvial architecture: an example from the Palaeocene–Eocene Bighorn Basin, Wyoming. *Sedimentology*, **64**, 1572–1596, https://doi.org/10.1111/sed.12364

Platt, N.H. and Keller, B. 1992. Distal alluvial deposits in a foreland basin setting —the Lower Freshwater Miocene), Switzerland: sedimentology, architecture and palaeosols. *Sedimentology*, **39**, 545–565, https://doi.org/10.1111/j.1365-3091.1992.tb02136.x

Potter, P. 1967. Sand bodies and sedimentary environments: a review. *AAPG Bulletin*, **3**, 337–365.

Powell, J.H. 2010. Jurassic sedimentation in the Cleveland Basin: a review. *Proceedings of the Yorkshire Geological Society*, **58**, 21–72, https://doi.org/10.1144/pygs.58.1.278

Pranter, M.J. and Sommer, N.K. 2011. Static connectivity of fluvial sandstones in a lower coastal-plain setting: an example from the Upper Cretaceous lower Williams Fork Formation, Piceance Basin, Colorado. *AAPG Bulletin*, **95**, 899–923, https://doi.org/10.1306/12091010008

Pranter, M.J., Cole, R.D., Panjaitan, H. and Sommer, N.K. 2009. Sandstone-body dimensions in a lower coastal-plain depositional setting: lower Williams Fork formation, Coal Canyon, Piceance Basin, Colorado. *AAPG Bulletin*, **93**, 1379–1401, https://doi.org/10.1306/06240908173

Pranter, M.J., Hewlett, A.C., Cole, R.D., Wang, H. and Gilman, J. 2014. Fluvial architecture and connectivity of the Williams Fork Formation: use of outcrop analogues for stratigraphic characterization and reservoir modelling. *Geological Society, London, Special Publications*, **387**, 57–83, https://doi.org/10.1144/SP387.1

Rahman, M.M. 2019. *Sedimentology and Characterization of Marginal Reservoir Facies in Fluvial and Delta Top Depositional Systems*. PhD thesis, University of Aberdeen, Aberdeen, UK.

Ravenne, C., Eschard, R., Galli, A., Mathieu, Y., Montadert, L. and Rudkiewicz, J.L. 1987. Heterogeneities and geometry of sedimentary bodies in a fluvio-deltaic reservoir. *SPE Formation Evaluation*, **4**, 239–246, https://doi.org/10.2118/16752-PA

Rawson, P.F. and Wright, J.K. 1992. *The Yorkshire Coast: The Yorkshire Coast Geologists' Association Guide no. 34*. The Geologists' Association, London, 1–117.

Riding, J.B. and Wright, J.K. 1989. Palynostratigraphy of the Scalby Formation (Middle Jurassic) of the Cleveland Basin, north-east Yorkshire. *Proceedings of the Yorkshire Geological Society*, **47**, 349–354, https://doi.org/10.1144/pygs.47.4.349

Rittersbacher, A., Howell, J.A. and Buckley, S.J. 2014. Analysis of fluvial architecture in the Blackhawk Formation, Wasatch Plateau, Utah, U.S.A., using large 3D photorealistic models. *Journal of Sedimentary Research*, **84**, 72–87, https://doi.org/10.2110/jsr.2014.12

Ryseth, A. 2000. Differential subsidence in the Ness Formation (Bajocian), Oseberg area, northern North Sea: facies variation, accommodation space development and sequence stratigraphy in a deltaic distributary system. *Norsk Geologisk Tidsskrift*, **80**, 9–25, https://doi.org/10.1080/002919600750042645

Sahoo, H., Gani, M.R. *et al.* 2020. Predictable patterns in stacking and distribution of channelized fluvial sand bodies linked to channel mobility and avulsion processes. *Geology*, **48**, 903–907, https://doi.org/10.1130/G47236.1

Sellwood, B.W. and Hallam, A. 1974. Bathonian volcanicity and North Sea rifting. *Nature, London*, **252**, 27–28, https://doi.org/10.1038/252027b0

Shanley, K.W. and McCabe, P.J. 1993. Alluvial architecture in a sequence stratigraphic framework: a case history from the Upper Cretaceous of southern Utah, U.S.A. *In*: Flint, S. and Bryant, I. (eds) *Quantative Modelling of Clastic Hydrocarbon Reservoirs and Outcrop Analogues*. International Association of Sedimentologists Special Publication, **15**, 21–55.

Shanley, K.W. and McCabe, P.J. 1994. Perspectives on the sequence stratigraphy of continental strata. *American Association of Petroleum Geologists Bulletin*, **78**, 544–568, https://doi.org/10.1306/BDFF9258-1718-11D7-8645000102C1865D

Slingerland, R. and Smith, N.D. 2004. River avulsions and their deposits. *Annual Review of Earth and Planetary Sciences*, **32**, 257–285, https://doi.org/10.1146/annurev.earth.32.101802.120201

Smith, R.M.H. 1993. Sedimentology and ichnology of floodplain paleosurfaces in the Beaufort Group (Late Permian), Karoo Sequence, South Africa. *Palaios*, **8**, 339–357, https://doi.org/10.2307/3515265

Smith, N.D. and Perez-Arlucea, M. 1994. Fine-grained splay deposition in the avulsion belt of the lower Saskatchewan River, Canada. *Journal of Sedimentary Research B: Stratigraphy & Global Studies*, **64**, 159–168, https://doi.org/10.1306/D4267F7D-2B26-11D7-8648000102C1865D

Smith, N.D., Cross, T.A., Dufficy, J.R. and Clough, S.R. 1989. Anatomy of an avulsion. 1–23.

Smith, D.G., Hubbard, S.M., Leckie, D.A. and Fustic, M. 2009. Counter point bar deposits: Lithofacies and reservoir significance in the meandering modern peace river and ancient McMurray formation, Alberta, Canada. *Sedimentology*, **56**, 1655–1669, 1165, https://doi.org/10.1111/j.1365-3091.2009.01050.x

Starmer, I.C. 1995. Deformation of the Upper Cretaceous Chalk at Selwicks Bay, Flamborough Head, Yorkshire: its significance in the structural evolution of north-east England and the North Sea Basin. *Proceedings of the Yorkshire Geological Society*, **50**, 213–228, https://doi.org/10.1144/pygs.50.3.213

Steel, R. and Aasheim, S.M. 1977. Alluvian Sand Deposition in a Rapidly Subsiding Basin (Devonian, Norway). *Canadian Society of Peteroleum Geologists*, **5**, 385–412.

Taylor, A.M. and Goldring, R. 1993. Description and analysis of bioturbation and ichnofabric. *Journal of the Geological Society*, **150**, 141–148, https://doi.org/10.1144/gsjgs.150.1.0141

Thomas, R.G., Smith, D.G., Wood, J.M., Visser, J., Calverley-range, E.A. and Koster, E.H. 1987. Inclined heterolithic stratification—terminology, description, interpretation and significance. *Sedimentary Geology*, **53**, 123–179, https://doi.org/10.1016/S0037-0738(87)80006-4

Tooth, S. 2005. Splay Formation along the lower reaches of ephemeral rivers on the northern plains of arid Central Australia. *Journal of Sedimentary Research*, **75**, 636–649, https://doi.org/10.2110/jsr.2005.052

Tyler, N. and Finley, R.J. 1991. Architectural controls on the recovery of hydrocarbons from sandstone reservoirs. In: Miall, A.D. and Tylers, C.N. (eds) *The Three Dimensional Facies Architecture of Heterogeneous Clastic Sediments and its Implications for Hydrocarbon Discovery and Recovery*. Concepts Sedimentol. Palontol., **3**, 44–54, https://doi.org/10.2110/csp.91.03.0001

Underhill, J.R. and Partington, M.A. 1993. Jurassic thermal doming and deflation in the North Sea: implications of the sequence stratigraphic evidence. *Geological Society, London, Petroleum Geology Conference Series*, **4**, 337–345, https://doi.org/10.1144/0040337

Van Toorenenburg, K.A., Donselaar, M.E., Noordijk, N.A. and Weltje, G.J. 2016. On the origin of crevasse-splay amalgamation in the Huesca fluvial fan (Ebro Basin, Spain): implications for connectivity in low net-to-gross fluvial deposits. *Sedimentary Geology*, **343**, 156–164, https://doi.org/10.1016/j.sedgeo.2016.08.008

Van Toorenenburg, K.A., Donselaar, M.E. and Weltje, G.J. 2018. The life cycle of crevasse splays as a key mechanism in the aggradation of alluvial ridges and river avulsion. *Earth Surface Processes and Landforms*, **43**, 2409–2420, https://doi.org/10.1002/esp.4404

Van Wagoner, J.C., Posamentier, H.W., Mitchum, R.M., Vail, P.R., Sarg, J.F., Loutit, T.S. and Hardenbol, J. 1988. An overview of the fundamentals of sequence stratigraphy and key definitions. *Sea-Level Changes: An Integrated Approach*, SEPM Special Publication, **42**, 39–45, https://doi.org/10.2110/pec.88.01.0039

Weissmann, G.S., Hartley, A.J., Nichols, G.J., Scuderi, L.A., Olson, M., Buehler, H. and Banteah, R. 2010. Fluvial form in modern continental sedimentary basins: distributive fluvial systems. *Geology*, **38**, 39–42, https://doi.org/10.1130/G30242.1

Weissmann, G.S., Hartley, A.J. *et al.* 2013. Prograding distributive fluvial systems – geomorphic models and ancient examples. *SEPM Special Publication*, **104**, 131–147, https://doi.org/10.2110/sepmsp.104.16

Widera, M. 2016. Depositional environments of overbank sedimentation in the lignite-bearing Grey Clays Member: new evidence from Middle Miocene deposits of central Poland. *Sedimentary Geology*, **335**, 150–165, https://doi.org/10.1016/j.sedgeo.2016.02.013

Willis, B.J. and Behrensmeyer, A.K. 1994. Architecture of Miocene overbank deposits in northern Pakistan. *Journal of Sedimentary Research*, **64**, 60–67, https://doi.org/10.1306/d4267f46-2b26-11d7-8648000102c1865d

Wood, J.M. 1985. *Sedimentology of the Late Cretaceous Judith River Formation, 'Cathedral' area, Dinosaur Provincial Park, Alberta*. MSc thesis, University of Calgary, Calgary, Alberta, 215.

Wood, J.M., Thomas, R.G. and Visser, J. 1988. Fluvial processes and vertebrate taphonomy: the upper cretaceous Judith River formation, South-Central dinosaur Provincial Park, Alberta, Canada. *Palaeogeography, Palaeoclimatology, Palaeoecology*, **66**, 127–143, https://doi.org/10.1016/0031-0182(88)90085-5

Wright, J.K. 2009. The geology of the Corallian ridge (Upper Jurassic) between Gilling East and North Grimston, Howardian Hills, North Yorkshire. *Proceedings of the Yorkshire Geological Society*, **57**, 193–216, https://doi.org/10.1144/pygs.57.3-4.193

Wright, V.P. and Marriott, S.B. 1993. The sequence stratigraphy of fluvial depositional systems: the role of floodplain sediment storage. *Sedimentary Geology*, **86**, 203–210, https://doi.org/10.1016/0037-0738(93)90022-W

Ziegler, P.A. 1982. *Geological Atlas of Western and Central Europe*. Elsevier Science, Amsterdam.